AD-A104 055 NAVAL POSTGRADUATE SCHOOL MONTEREY CA F/G 20/4
FREE CONVECTION FROM A SEMI-INFINITE VERTICAL PLATE WITH DISCON--ETC(U)
MAR 81 W A SCHIESSER

UNCLASSIFIED NL

1 OF 2
AD
A104055

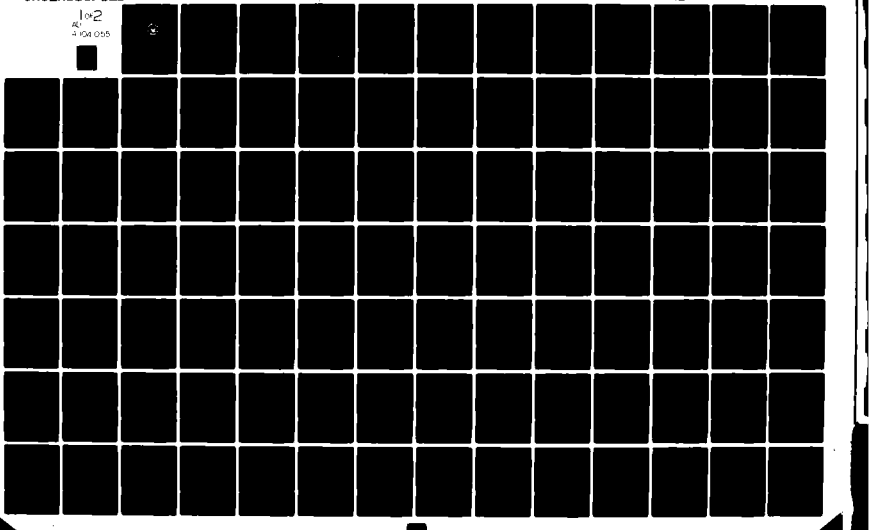

NAVAL POSTGRADUATE SCHOOL

Monterey, California

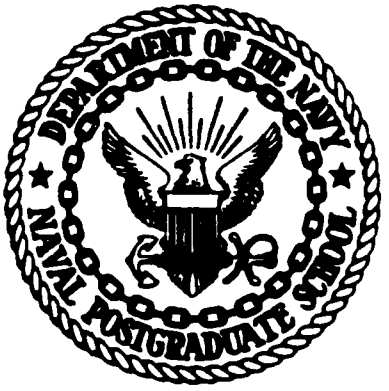

THESIS

FREE CONVECTION FROM A SEMI-INFINITE VERTICAL PLATE WITH DISCONTINUOUS BLOWING OR SUCTION

by

William Andrew Schiesser

March 1981

Thesis Advisor: M.D. Kelleher

Approved for public release, distribution unlimited

Unclassified

SECURITY CLASSIFICATION OF THIS PAGE (When Data Entered)

REPORT DOCUMENTATION PAGE	READ INSTRUCTIONS BEFORE COMPLETING FORM
1. REPORT NUMBER	2. GOVT ACCESSION NO. AD-A104 055 / 3. RECIPIENT'S CATALOG NUMBER
4. TITLE (and Subtitle) Free Convection from a Semi-Infinite Vertical Plate with Discontinuous Blowing or Suction	5. TYPE OF REPORT & PERIOD COVERED Master's/Engineer Thesis March 1981
	6. PERFORMING ORG. REPORT NUMBER
7. AUTHOR(s) William Andrew Schiesser	8. CONTRACT OR GRANT NUMBER(s)
9. PERFORMING ORGANIZATION NAME AND ADDRESS Naval Postgraduate School Monterey, California 93940	10. PROGRAM ELEMENT, PROJECT, TASK AREA & WORK UNIT NUMBERS
11. CONTROLLING OFFICE NAME AND ADDRESS Naval Postgraduate School Monterey, California 93940	12. REPORT DATE March 1981
	13. NUMBER OF PAGES 108
14. MONITORING AGENCY NAME & ADDRESS(if different from Controlling Office)	15. SECURITY CLASS. (of this report)
	15a. DECLASSIFICATION/DOWNGRADING SCHEDULE

16. DISTRIBUTION STATEMENT (of this Report)

Approved for public release, distribution unlimited.

17. DISTRIBUTION STATEMENT (of the abstract entered in Block 20, if different from Report)

18. SUPPLEMENTARY NOTES

19. KEY WORDS (Continue on reverse side if necessary and identify by block number)

Free convection,
Discontinuous suction and blowing

20. ABSTRACT (Continue on reverse side if necessary and identify by block number)

An analytical investigation of laminar free convection from a semi-infinite vertical plate is undertaken with the following special conditions imposed. The plate is maintained at a constant temperature greater than that of the ambient fluid. At an arbitrary distance above the leading edge a constant rate of blowing or suction is initiated extending uniformly along the remainder of the plate. The solution was obtained using the

DD FORM 1 JAN 73 1473 EDITION OF 1 NOV 65 IS OBSOLETE
S/N 0102-014-6601

Unclassified
SECURITY CLASSIFICATION OF THIS PAGE (When Data Entered)

Item 20 continued:

method of matched asymptotic expansions whereby an inner series described the velocity and temperature profiles near the discontinuity in the vicinity of surface and an outer series approximated the behavior at greater distances from the plate. The inner series was also used to determine the heat transfer characteristics at the surface of the plate. The ambient fluid was assumed to be air with a Prandtl number of 0.72.

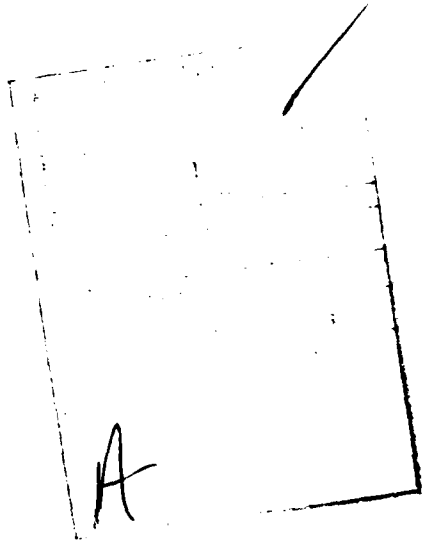

Approved for public release; distribution unlimited.

Free Convection from a Semi-Infinite Vertical Plate with Discontinuous Blowing or Suction

by

William Andrew Schiesser
Lieutenant Commander, U.S. Navy
B.A., Knox College, 1969
M.A., University of Wisconsin, 1971

Submitted in partial fulfillment of the requirements for the degree of

MASTER OF SCIENCE IN MECHANICAL ENGINEERING

from the

NAVAL POSTGRADUATE SCHOOL

March 1981

Author: William A. Schiesser

Approved by: Whitchin-Killen
Thesis Advisor

Benjamin Gebhart
Second Reader

P. J. Marto
Chairman, Department of Mechanical Engineering

William M. Tolles
Dean of Science and Engineering

ABSTRACT

An analytical investigation of laminar free convection from a semi-infinite vertical plate is undertaken with the following special conditions imposed. The plate is maintained at a constant temperature greater than that of the ambient fluid. At an arbitrary distance above the leading edge a constant rate of blowing or suction is initiated extending uniformly along the remainder of the plate. The solution was obtained using the method of matched asymptotic expansions whereby an inner series described the velocity and temperature profiles near the discontinuity in the vicinity of surface and an outer series approximated the behavior at greater distances from the plate. The inner series was also used to determine the heat transfer characteristics at the surface of the plate. The ambient fluid was assumed to be air with a Prandtl number of 0.72.

TABLE OF CONTENTS

LIST OF SYMBOLS

A_1, A_2, B_1, B_1^*, C_1, C_1^*, etc.	Constant coefficients in the asymptotic forms for f_k and g_k defined in equations (D-1)
a_n, b_n	Constant coefficients in the initial free convection series approximations for F and H defined in equations (A-4)
c_p	Specific heat at constant pressure (j/kg^oK)
F	Stream function in the similar free convection equations
f_k	Coefficient functions of the inner series expansion for ψ
Gr	Grashof number based on L, $Gr = \frac{g\beta(\overline{T}_w - \overline{T}_\infty)L^3}{\nu^2}$
Gr*	Grashof number based on $\overline{x} + L$, the length scale with respect to the leading edge, $Gr^* = \frac{g\beta(\overline{T}_w - \overline{T}_\infty)(\overline{x} + L)^3}{\nu^2}$
g	Gravitational acceleration (m/s^2)

g_k	Coefficient functions of inner series expansion for θ
H	Dimensionless temperature variable in the similar free convection equations
k	Thermal conductivity (W/m.^{o}k)
L	Distance above the leading edge at which blowing or suction begins (m)
$Nu(Gr/4)^{-\frac{1}{4}}$	Heat transfer parameter at the surface of the plate with discontinuous suction or blowing applied defined in equation (48)
$Nu_0(Gr/4)^{-\frac{1}{4}}$	Heat transfer parameter at the surface of the plate in the case of unperturbed free convection defined in equation (47)
$Nu_1(Gr/4)^{-\frac{1}{4}}$	Heat transfer parameter at the surface of the plate in the case of continuous blowing or suction defined in equation (49)
Pr	Prandtl number of the ambient fluid
q''_0	Local heat flux at the surface of the plate (W/m^2)
$\bar{T}_w$	Temperature of the plate (^{o}C)
$\bar{T}_\infty$	Temperature of the ambient fluid (^{o}C)

$\bar{u}$	Streamwise velocity (m/s)
$\bar{u}_{max}$	Maximum value of the streamwise velocity in the free convection case (m/s)
u	Nondimensional streamwise velocity defined in equation (4c)
u*	stretched nondimensional streamwise velocity difined in equation (5b)
$\bar{v}$	Velocity normal to the plate (m/s)
$\bar{v}_w$	Suction or blowing velocity applied normal to the plate at its surface (m/s)
v	Nondimensional velocity normal to the plate defined in equation (4d)
v*	Stretched nondimensional velocity normal to the plate defined in equation (5c)
Y_{10}, Y_{11}, Y_{20}, etc.	Universal functions used in solving for the inner series coefficient functions, f_k, defined in equations (22)
$\bar{x}$	Dimensional distance in the stream-wise direction (m)
x	Nondimensional distance in the stream-wise direction defined in equation (4a)

$\bar{y}$	Dimensional distance normal to the plate (m)
y	Nondimensional distance normal to the plate defined in equation (4b)
y^*	Stretched nondimensional distance normal to the plate defined in equation (5a)
Z_{10}, Z_{11}, etc.	Universal functions used in solving for the inner series coefficient functions, g_k, defined in equations (22)
α	Thermal diffusivity (m^2/s)
β	Coefficient of volumetric expansion ($^oK^{-1}$)
γ	Matching point for inner and outer expansions defined in equation (D-3)
η	Local similarity variable for the inner series expansions defined in equation (16)
η_F	Free convection similarity variable defined in equation (11)
η_{end}	End-point of numerical integration
ϵ^*	Nondimensional blowing/suction parameter defined in equation (8b)
ξ	Local streamwise similarity variable

	for the inner and outer expansions defined in equation (16)
ξ_1	Sparrow and Cess parameter defined in equation (48)
ν	Kinematic viscosity (m^2/s)
ψ	Nondimensional stream function defined in equation (15a)
ψ_1, ψ_2, etc.	Coefficient functions for ψ in the outer series expansion defined in equation (34)
θ	Nondimensional temperature distribution defined in equations (4e)
θ_1, θ_2, etc.	The coefficient functions for the outer series expansion of θ defined in equations (35)

ACKNOWLEDGEMENTS

The author wishes to acknowledge the valuable assistance, guidance, and encouragement given by his advisor, Professor Matthew D. Kelleher. His patience and accessability throughout the entire duration of this research project were instrumental in its successful completion. Also, the author wishes to thank Professor Benjamin Gebhart, for his very helpful comments and suggestions. For her conscientious and professional efforts in typing the final manuscript, the author wishes to thank Mrs. Edna Cerone.

The W.R. Church Computer Center at the Naval Postgraduate School provided facilities for all of the computer work.

I. INTRODUCTION

The study of free convection has been the subject of ongoing research over the past century both from an analytical and experimental point of view. An excellent overview of the progress made in this area can be found in Ede [1]. Two outstanding expositions of the fundamentals of heat transfer by the mechanism of free convection are presented by Gebhart [2] and Moore [3].

The technique of solving boundary layer problems by employing similarity analysis is discussed in general by Hansen [4] and specific applications of the method are presented by Yang [5].

The problem discussed in this paper is that of an analytical investigation of the effects of blowing and suction applied at a specified distance above the leading edge of a uniformly heated semi-infinite vertical plate on the heat transfer characteristics at the surface of the plate.

An early study of the effects of mass transfer on free convection was conducted by Eichhorn [6] who showed that similar solutions are possible for blowing or suction rate distributions which vary as the distance from the leading edge of the plate raised to a power related to the variation in surface temperature.

Since the prescribed surface temperature itself varied as a power of the distance from the leading edge, this proved to be a somewhat restricted case of limited physical application. The case of a uniformly heated plate with constant blowing or suction along the entire extent of the surface was succinctly treated by Sparrow and Cess [7] who extended their analysis to include independent power law variations of both surface temperature and mass transfer. Their analysis which was based on an asymptotic series expansion of the stream function and temperature distribution evaluated the first order effects of blowing and suction on free convection. An extension of this work to include possible variations in the fluid properties was conducted by Parikh, Kays and Bershader [8] who employed a numerical finite difference scheme to solve the resulting equations. Their numerical predictions were in close agreement with interferometric data obtained through their own experiments. The results of these authors and especially those reported by Sparrow and Cess have been of great value in affording a comparison with results obtained in the present study. A comprehensive investigation of the effects of suction and blowing on heat transfer and wall skin friction which included regions on the plate at large distances from the leading edge was conducted by Merkin [9]. In that analysis a step-by-step numerical solution of the boundary layer equations begins at the leading edge and proceeds systematically up the plate until the asymptotic velocity

and temeperature profiles are obtained to whatever accuracy is required.

There have been several additional studies in the area of free convection past a vertical plate with various conditions of wall temperature or heat flux and imposed variations in transpiration at the surface of the plate. An analysis which transformed the laminar boundary layer equations resulting from arbitrary distributions in both wall temperature and blowing into ordinary differential equations with variable coefficients and constant boundary conditions was presented by Vedhanayagan, Altenkirch, and Eichhorn [10]. In the area of unsteady free convection where either the plate surface temperature or transpiration rate varies with time there have been at least four notable studies during the past twenty years. Nanda and Sharma [11] undertook analytical investigations and determined that similarity solutions were possible for the following two cases: surface temperature varying as some power of time and suction velocity varying as time to the minus one-half power; and the second case where surface temperature is an exponential or periodic function of time and the suction velocity is constant. The effects of mass diffusion on the unsteady free convective flow past a simi-infinite porous plate with constant suction were studied through mathematical analysis by Soundalgekar and Wavre [12]. With the assumption that the plate temperature oscillated in time about a constant mean, approximate

solutions were derived for the mean flow, transient flow, the amplitude and phase of the skin friction and the rate of heat transfer. The effects of the nondemensional parameters Grashof number, Prandtl number, Eckert number and Schmidt number were also reported. The most general unsteady situation where both wall temperature and suction velocity are periodic functions of time was considered by Lal [13]. All of the previous studies cited have neglected the effects of viscous dissipation; however, this effect is not insignificant when the natural convection flow field is very large or the flow occurs in the presence of extremely low temperatures or very high gravity fields. The combined effect of viscous dissipation with the suction velocity and plate temperature oscillating at the same frequency on free convection past a vertical plate was analyzed by Soundalgekar and Pop [14]. In their study expressions for the mean velocity, transient velocity, transient temperature profiles, amplitude and phase of skin friction and the rate of heat transfer were derived and the results compared to those reported for the case of constant suction velocity.

A review of the literature in the field of free convection on a vertical plate clearly indicates a desire on the part of researchers to investigate perturbations of the thermal and momentum boundary layers resulting from the introduction of temperature or velocity discontinuities along the surface of the plate and their ultimate effect on skin friction and

heat transfer at the wall. The specific nature of the discontinuity will determine the manner in which the perturbation effects propagate through the boundary-layers and; therefore, will often indicate a preferred method of analytical solution. Although there are several possible mathematical techniques available to researchers in this field, two fundamentally different approaches predeminate, each with numerous variations. An example of the finite difference method of solution to the boundary-layer equations resulting from a discontinuity in the surface wall temperature can be found in Na [15]and Meena and Nath [16]. This technique has gained in acceptance with the advent of larger and faster digital computers. The other major technique involves the expansion of both the stream function and temperature profile in an asymptotic series. The original proponent of this method was Goldstein who presented the details of the asymptotic series technique, commonly known as the Goldstein series, in [17]. After reducing the set of governing boundary-layer equations by the introduction of a stream function such that:

$$u = \frac{\partial \psi}{\partial y} \text{ and } v = \frac{-\partial \psi}{\partial x}$$

two new variables are introduced which are of the following general form:

1) In the streamwise direction: $\xi = x^{\frac{1}{n}}$

2) In the direction normal to the plate: $\eta = yx^{-1/n}$

A series is then formed in powers of ξ for the stream function and temperature distribution with undetermined coefficient

functions f_k, g_k respectively which depend only on η. The problem is then finally reduced to one of determining the coefficient functions; the solution of a fifth order set of linear coupled ordinary differential equations for each pair of coefficients subject to the appropriate boundary conditions. This technique is especially powerful when employed to investigate conditions at or near the surface of the plate. In order to examine the laminar free convection wake above a heated vertical plate Yang [18] successfully employed this technique to obtain detailed velocity and temperature profiles in the immediate vicinity of the trailing edge and then expanded these results to the rest of the wake by an integral solution. Another example of this technique is found in Kelleher [19] where a step discontinuity in the surface temperature imposed at a finite distance above the leading edge of the plate caused a perturbation of both the thermal and momentum boundary-layers. An inner expansion of the Goldstein type was employed to obtain the behavior of heat transfer near the surface of the plate and an outer asymptotic series expansion was constructed to determine the velocity and temperature profiles at greater distances from the plate. A similar approach is employed to analytically investigate the present problem where a discontinuity in the velocity boundary condition is propagated through the momentum and thermal boundary-layers. Laminar flow is assumed as are constant transport properties of the ambient fluid. The

primary aim of the study is the determination of any enhancement or degradation of the heat transfer rate at the surface of the plate compared to the same plate without blowing or suction over the entire length.

II. ANALYSIS

A. COORDINATE SYSTEM

The problem considered in this paper is that of laminar free convective flow from a uniformly heated semi-infinite vertical plate with leading edge oriented downward in a standard gravitational field. A constant rate of blowing or suction is applied at the surface beginning at an arbitrary distance, L, above the leading edge. A rectangular cartesian coordinate system with origin as indicated in Figure 1 was employed in the analysis. As is indicated throughout the paper various transformations of the basic coordinates are invoked to facilitate the solution of the problem.

B. GOVERNING EQUATIONS

The analysis is based on the standard Boussinesq free convection approximation which assumes that only density variations giving rise to buoyant forces are considered with the effects of viscous dissipation neglected. With these standard assumptions the two dimensional equations of continuity, momentum, and energy boundary-layer form are:

$$\frac{\partial \bar{u}}{\partial \bar{x}} + \frac{\partial \bar{v}}{\partial \bar{y}} = 0 \tag{1}$$

$$\bar{u} \frac{\partial \bar{u}}{\partial \bar{x}} + \bar{v} \frac{\partial \bar{u}}{\partial \bar{y}} = \nu \frac{\partial^2 \bar{u}}{\partial \bar{y}^2} + g\beta(\bar{T} - \bar{T}_\infty) \tag{2}$$

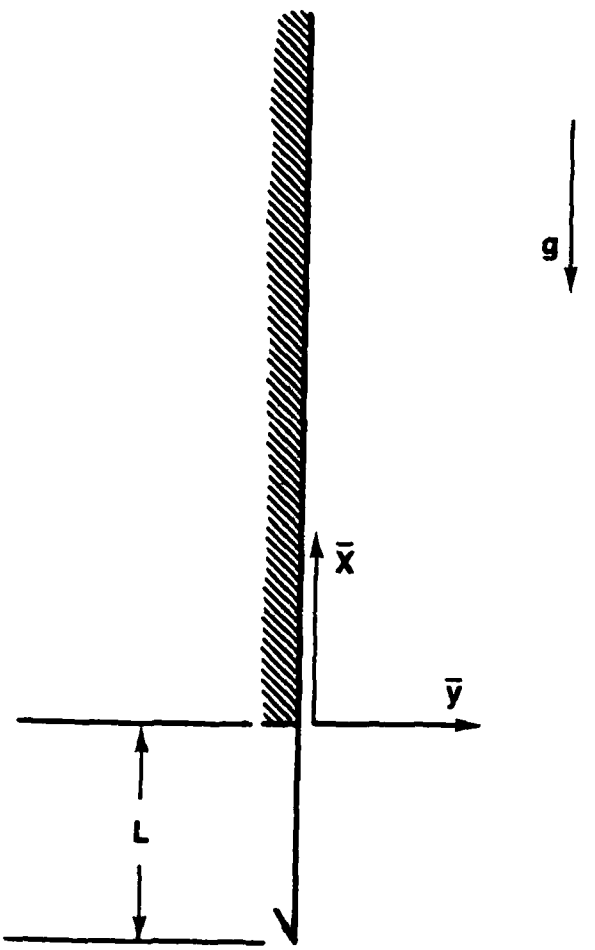

Figure 1: Basic Coordinate System

$$\bar{u}\frac{\partial \bar{T}}{\partial \bar{x}} + \bar{v}\frac{\partial \bar{T}}{\partial \bar{y}} = \alpha \frac{\partial^2 \bar{T}}{\partial \bar{y}^2} \tag{3}$$

where $\bar{T}_\infty$ is the constant ambient fluid temperature. These equations must also satisfy the following physical boundary conditions:

$$\begin{aligned} &\text{At } \bar{y} = 0: \quad \bar{u} = 0 \\ &\qquad\qquad \bar{v} = \bar{v}_w, \qquad \bar{x}>0 \\ &\qquad\qquad \bar{v} = 0, \qquad -L<\bar{x}<0 \\ &\qquad\qquad \bar{T} = \bar{T}_w \\ &\text{and as } \bar{y} \to \infty: \quad \bar{u} = 0 \\ &\qquad\qquad \bar{T} = \bar{T}_\infty \end{aligned} \tag{3a}$$

The non-zero normal velocity boundary condition at $\bar{x} = 0$ and $\bar{y} = 0$ introduces a discontinuity into the boundary-layer equations which has a primary direct effect on the formation of the momentum boundary-layer and a secondary influence on the development of the thermal boundary-layer. A positive value for v_w will represent the blowing of fluid away from the wall and a negative value for v_w will represent the suction of fluid through the plate.

In order to facilitate the analysis, the variables in equations (1)-(3) are non-dimensionalized according to the following transformations:

$$x = \frac{\bar{x}}{L} \tag{4a}$$

$$y = \frac{\bar{y}}{L} \tag{4b}$$

$$u = \frac{\bar{u}L}{\nu} \tag{4c}$$

$$v = \frac{\bar{v}L}{\nu} \tag{4d}$$

$$\theta = \frac{\bar{T} - \bar{T}_\infty}{\bar{T}_w - \bar{T}_\infty} \tag{4e}$$

where L is the distance above the leading edge where suction or blowing commences, and $\bar{T}_w$ is the constant wall temperature. The equations are further simplified through the introduction of the conventional stream function ψ and by stretching y, u, and v as follows:

$$y^* = y\left(\frac{Gr}{4}\right)^{\frac{1}{4}} \tag{5a}$$

$$u^* = u(4Gr)^{-\frac{1}{2}} = \frac{\partial \psi}{\partial y^*} \tag{5b}$$

$$v^* = v(64Gr)^{-\frac{1}{4}} = -\frac{\partial \psi}{\partial x} \tag{5c}$$

where the Grashof number, Gr, is evaluated with respect to L, the length scale associated with the discontinuity. It should be noted that this length scale is not the conventional one used in free convection problems where distance from the leading edge is normally used to evaluate Gr. Now after substituting equations (5) into equations (1)-(3), the continuity equation is eliminated and the momentum and energy equations reduce to the following:

$$4\frac{\partial \psi}{\partial y^*} \cdot \frac{\partial^2 \psi}{\partial x \partial y^*} - 4\frac{\partial \psi}{\partial x} \cdot \frac{\partial^2 \psi}{\partial y^{*2}} = \frac{\partial^3 \psi}{\partial y^{*3}} + \theta \tag{6}$$

$$4 \frac{\partial \psi}{\partial y^*} \frac{\partial \theta}{\partial x} - 4 \frac{\partial \psi}{\partial x} \frac{\partial \theta}{\partial y^*} = \frac{1}{Pr} \frac{\partial^2 \theta}{\partial y^{*2}} \tag{7}$$

The non-zero normal velocity component imposed at the surface of the plate perturbs the governing equations (6) and (7) precluding the existence of a similarity solution. Therefore, an approximate solution to these equations will be obtained by means of inner and outer asymptotic series expansions for both ψ and θ. The inner expansions will approximate local behavior near the surface of the plate in the vicinity of the discontinuity, and the outer expansions will model velocity and temperature profiles at greater distances from the plate.

C. BOUNDARY AND INITIAL CONDITIONS

The nondimensional form of the governing equations given in (6) and (7) must satisfy the original physical boundary conditions as specified in (3a) which reduce to the following conditions in terms of the stream function ψ and temperature distribution Θ:

$$\begin{aligned}
&\text{At } y^* = 0: \quad u^* = \frac{\partial \psi}{\partial y^*} = 0 \\
&\qquad\qquad\quad v^* = -\frac{\partial \psi}{\partial x} = \pm \varepsilon^* \,, \quad x > 0 \\
&\qquad\qquad\quad v^* = -\frac{\partial \psi}{\partial x} = 0, \quad -L < x < 0 \\
&\qquad\qquad\quad \Theta = 1 \\
&\text{As } y^* \to \infty: \quad u^* = 0 \\
&\qquad\qquad\quad \Theta = 0
\end{aligned} \tag{8a}$$

where ε^* is related to the physical blowing or suction rate, $\bar{v}_w$, by the following:

$$\varepsilon^* = \frac{-v_w L}{\nu} (64Gr)^{-\frac{1}{4}} \tag{3b}$$

Since this problem involves a perturbation of both the momentum and thermal boundary-layers which began developing at the leading edge, the initial conditions at the origin of the discontinuity, i.e., x = 0, must match these free convection profiles. For a semi-infinite vertical plate maintained at a constant temperature the following ordinary differential equations describe unperturbed free convection behavior:

$$F''' + 3FF'' - 2F'^2 + H = 0 \tag{9a}$$

$$\frac{1}{Pr} H'' + 3FH' = 0 \tag{9b}$$

with the following boundary conditions:

$$\begin{aligned} &\text{At} \quad \eta = 0: \quad F(0) = F'(0) \; ; \; H(0) = 1 \\ &\text{As} \quad \eta \to \infty: \quad F'(\infty) = 0; \; H(\infty) = 0 \end{aligned} \tag{10}$$

where F is the similarity stream function and H is the dimensionless temperature distribution and primes indicate derivatives with respect to the free convection similarity variable η_f defined as follows:

$$\eta_f = \frac{\bar{y}}{(\bar{x}+L)} \left(\frac{Gr^*}{4}\right)^{\frac{1}{4}} \tag{11}$$

where Gr* is evaluated at $\bar{x}$+L according to the free convection length scale which has its origin at the leading edge. It should be noted that all references or comparisons to the unperturbed free convection problem employ this translated length scale, whereas the length scale for the perturbed problem is based on L with origin at $\bar{x}$ = 0. At $\bar{x}$ =0 equation (11) reduces to $\eta_f = y^*$. The solution to the equations (9) are well known; however, an excellent summary of solutions for this and other more general cases can be found in Yang [5].

Since the initial length of the plate is unperturbed, the velocity and temperature profiles at x = 0 will be given by the following:

$$u = (4Gr)^{\frac{1}{2}} F'(y^*) \tag{12a}$$

$$\Theta = H(y^*) \tag{12b}$$

Therefore, the initial velocity and temperature profiles originating at x = 0 must match those obtained from equations (12). The details of expressing F and H in a form which will permit this matching condition to be mathematically formulated are presented in Appendix A.

III. METHOD OF SOLUTION

A. REDUCTION OF THE GOVERNING EQUATIONS

The nondimensional forms of the governing equations for the problem under consideration are:

$$4\frac{\partial\psi}{\partial y^*}\frac{\partial^2\psi}{\partial x\partial y^*} - 4\frac{\partial\psi}{\partial x}\frac{\partial^2\psi}{\partial y^{*2}} = \frac{\partial^3\psi}{\partial y^{*3}} + \theta \tag{6}$$

$$4\frac{\partial\psi}{\partial y^*}\frac{\partial\theta}{\partial x} - 4\frac{\partial\psi}{\partial x}\cdot\frac{\partial\theta}{\partial y^*} = \frac{1}{Pr}\frac{\partial^2\theta}{\partial y^{*2}} \tag{7}$$

In order to apply the Goldstein series method of solution to these equations suitable expansions of ψ and θ must be constructed of the following form:

$$\psi = \varepsilon^*(\xi/\phi_1)^{\frac{1}{a}} + \phi_3\xi^c[\xi^k f_k(\eta)] \tag{13}$$

and $$\theta = 1 + \phi_4\xi^d[\xi^k g_k(\eta)] \tag{14}$$

where $\xi = \phi_1 x^a$; $\eta = \phi_2 y^* x^b$; the ϕ's are possibly functions of ε^*; and the a, b, c, d are constants to be determined. The following conditions must be satisfied which impose certain restrictions on the ϕ's and exponent constants:

1) The u velocities from the free convection region ($\bar{x}<0$) and from the perturbed stream function, i.e., $u^* = \frac{\partial\psi}{\partial y^*}$, must match at $\bar{x} = 0$.
2) The temperature profiles must match at $\bar{x} = 0$.
3) The highest order derivative of the coefficient functions must appear in the zeroth order expansions which

result upon substitution of equations (13) and (14) into equations (6) and (7).

4) The exponent constants in the expansions referred to in 3) above must be integers.

The details of applying the conditions outlined above to determine the unknown parameters are presented in Appendix B along with the boundary conditions which must be satisfied by the coefficient functions f_k and g_k.

Using the results of Appendix B equations (13) and (14) are transformed into the following:

$$\psi = \frac{4}{3}\varepsilon^*\xi^3 + \xi^2[\xi^k f_k] \tag{15a}$$

and $$\theta = 1 + \xi[\xi^k g_k] \tag{15b}$$

where $\xi = (\frac{3}{4}x)^{1/3}$ and $\eta = (\frac{3}{4}x)^{-1/3}y^* = y^*/\xi$. (16)

The momentum and energy equations (6) and (7) are transformed into:

$$[(k+1)\xi^k f_k'][\xi^k f_k'] - [(k+2)\xi^k f_k][\xi^k f_k''] - 4\varepsilon^*\xi[\xi^k f_k'] = [\xi^k f_k'''] + \xi + \xi^2[\xi^k g_k] \tag{17}$$

and $$[(k+1)\xi^k g_k][\xi^k f_k'] - [(k+2)\xi^k f_k][\xi^k g_k'] - 4\varepsilon^*\xi[\xi^k g_k'] = \frac{1}{Pr}[\xi^k g_k''] \tag{18}$$

where the repeated index k indicates the standard Einstein summation. By the process of equating coefficients of like powers of ξ the following ordinary differential equations involving the coefficient functions are obtained.

Momentum Equation:

$$\text{0th order:} \quad f_0''' + 2f_0 f_0'' - f_0'^2 = 0$$

$$\text{1st order:} \quad f_1''' + 2f_0 f_1'' - 3f_0' f_1' + 3f_0'' f_1 = -4\varepsilon^* f_0'' - 1 \qquad (19)$$

$$\text{2nd order:} \quad f_2''' + 2f_0 f_2'' - 4f_0' f_2' + 4f_0'' f_2 = 2f_1'^2 - 3f_1 f_1'' - 4\varepsilon^* f_1'' - g_0$$

Energy Equation:

$$\text{0th order:} \quad \frac{1}{Pr} g_0'' + 2f_0 g_0' - f_0' g_0 = 0$$

$$\text{1st order:} \quad \frac{1}{Pr} g_1'' + 2f g_1' - 2f' g_1 + 3g_0' f_1 - g f_1' = -4\varepsilon^* g_0' \qquad (20)$$

$$\text{2nd order:} \quad \frac{1}{Pr} g_2'' + 2f_0 g_2' - 3f_0' g_2 + 4g_0' f_2 - g_0 f_2' = 2g_1 f_1' - 3g_1' f_1 - 4\varepsilon^* g_1'$$

From Appendix B the following boundary conditions must be satisfied by the zeroth order momentum and energy equations:

At $\eta = 0$: $\quad f_0(0) = f_0'(0) = g_0(0) = 0$

As $\eta \to \infty$: $\quad \frac{f_0'}{\eta} = 2a_2 ; \frac{g_0}{\eta} = b_1$

where $a_2 = \frac{1}{2}F''(0)$ and $b_1 = H'(0)$.

The solutions of the zeroth order equations are now straightforward and yield the following:

$$f_0 = a_2 \eta^2 \qquad (21a)$$

and $$g_0 = b_1 \eta \qquad (21b)$$

B. DETERMINATION OF THE HIGHER ORDER COEFFICIENT FUNCTIONS

The first and higher order coefficient functions f_k, and g_k for the stream function and temperature distribution inner expansions are obtained by solving the sets of coupled fifth

order ordinary differential equations (19) and (20). These equations were obtained by equating like powers of ξ in the momentum and energy expansion defined in equations (17) and (18). The presence of ε^* in the inhomogeneous parts of the differential equations introduces another independent parameter which significantly complicates the numerical procedure employed in their solution. To eliminate this problem and isolate the effects of ε^* the coefficient functions can be redefined in terms of universal functions which depend only on the Prandtl number. The revised forms of f_k and g_k appear in equations (22), presented below.

$$
\begin{aligned}
f_1 &= Y_{10} + \varepsilon^* Y_{11} \\
g_1 &= Z_{10} + \varepsilon^* Z_{11} \\
f_1 &= Y_{20} + \varepsilon^* Y_{21} + \varepsilon^{*2} Y_{22} \\
g_2 &= Z_{20} + \varepsilon^* Z_{21} + \varepsilon^{*2} Z_{22}
\end{aligned}
\tag{22}
$$

where the Y_{10}, Z_{10}, etc. are universal functions of η depending only on the Prandtl number. Since the first and higher order equations of (19) and (20) are linear, the principle of superposition applies and the equations of (22) can be substituted into (17) and (18) and separate like power of ε^* and obtain the following equations.

The first order momentum equation becomes:

$$M_1[Y_{10}] = -1 \tag{23a}$$

and $$M_1[Y_{11}] = -4f_0'', \tag{23b}$$

where M_1 is the linear differential operator defined by:

$$M_1 = Y_1''' + 2f_0 Y_1'' - 3f_0' Y_1' + 3f_0'' Y_1 \tag{23c}$$

The first order energy equation becomes:

$$E_1[Z_{10}] = 0 \tag{24a}$$

and $$E_1[Z_{11}] = -4Z'_{00}, \tag{24b}$$

where E_1 is the linear differential operator defined by:

$$E_1 = \frac{1}{Pr}Z''_1 + 2f_0Z'_1 - 2f'_0Z_1 + 3Z'_{00}Y_1 - Z_{00}Y'_1 \tag{24c}$$

The second order momentum equation becomes:

$$M_2[Y_{20}] = 2Y'^2_{10} - 3Y_{10}Y''_{10} - Z_{00}; \tag{25a}$$

$$M_2[Y_{21}] = 4Y'_{10}Y'_{11} - 3Y_{10}Y''_{11} - 3Y_{11}Y''_{10} - 4Y''_{10}; \tag{25b}$$

and $$M_2[Y_{22}] = 2Y'^2_{11} - 3Y_{11}Y''_{11} - 4Y''_{11}, \tag{25c}$$

where M_2 is the linear differential operator defined by:

$$M_2 = Y'''_2 + 2f_0Y''_2 - 4f'_0Y'_2 + 4f''_0Y_2. \tag{25d}$$

The second order energy equation becomes:

$$E_2[Z_{20}] = 2Y'_{10}Z_{10} - 3Y_{10}Z'_{10}; \tag{26a}$$

$$E_2[Z_{21}] = 2Y'_{10}Z_{11} + 2Y'_{11}Z_{10} - 3Y_{10}Z'_{11} - 3Y_{11}Z'_{10} - 4Z'_{10}; \tag{26b}$$

and $$E_2[Z_{22}] = 2Y'_{11}Z_{11} - 3Y_{11}Z'_{11} - 4Z'_{11}, \tag{26c}$$

where E_2 is the linear differential operator defined by:

$$E_2 = \frac{1}{Pr}Z''_2 + 2f_0Z'_2 - 3f'_0Z_2 + 4Z'_2Y_2 - Z_{00}Y'_2 \tag{26d}$$

The following boundary conditions must be satisfied by equations (23)-(26):

At $\eta = 0$: $$Y_{10} = Y_{11} = Y_{20} = Y_{21} = Y_{22} = 0;$$
$$Y'_{10} = Y'_{11} = Y'_{20} = Y'_{21} = Y'_{22} = 0; \tag{27}$$
and $$Z_{10} = Z_{11} = Z_{20} = Z_{21} = Z_{22} = 0;$$

As $\eta \to \infty$: $$\frac{Y'_{10}}{\eta^2} \to -\tfrac{1}{2}, \quad Y'_{11} \to 0$$

$$\frac{Y'_{20}}{\eta^3} \to \frac{-H'(0)}{6} \; ; \; Y'_{21} \to 0, \; Y'_{22} \to 0;$$

$$\frac{Z_{10}}{\eta^2} \to 0, \; Z_{21} \to 0; \tag{28}$$

and

$$\frac{Z_{20}}{\eta^3} \to 0, \; Z_{21} \to 0, \; Z_{22} \to 0$$

which follow directly from the coefficient function boundary conditions given in equations (B-33), (B-35) and B-36).

Although they were not used in the present analysis, the third order universal function equations are presented in Appendix C.

C. CONSTRUCTION OF THE OUTER SERIES EXPANSIONS

The inner series developed in the preceding section is useful only in approximating local behavior at the surface in the vicinity of the discontinuity. In order to describe the temperature and velocity profiles at greater distances from the plate another series is required which will satisfy the asymptotic boundary conditions and also match the inner series at some intermediate distance from the surface. According to the method of Goldstein [17] the outer series expansions for the stream function and temperature distribution should be of the following form:

$$\psi = \psi_0(Y^*) + \xi\psi_1(Y^*) + \frac{1}{2!}\xi^2\psi_2(Y^*) + \frac{1}{3!}\xi^3\psi_3(Y^*) \tag{29}$$

and

$$\theta = \theta_0(Y^*) + \xi\theta_1(Y^*) + \frac{1}{2!}\xi^2\theta_2(Y^*) + \frac{1}{3!}\xi^3\theta_3(Y^*) \tag{30}$$

Since as $\xi \to 0$ the original initial conditions must be satisfied, the following equalities must hold; thus defining the zeroth order coefficients:

$$\psi_0(y^*) = F(y^*)$$

and

$$\theta_0(y^*) = H(y^*) \tag{31}$$

where F and H are the free convection similarity functions for the stream function and temperature distribution, respectively. This condition is merely a mathematical restatement of the physical condition which requires that the temperature and velocity profiles at the discontinuity, $\xi = 0$, match those generated by the free convection process in the region between the leading edge and the discontinuity.

Now the asymptotic outer series froms (29) and (30) are substituted into the governing equations (6) and (7). Once again through the process of collecting terms which are coefficients of like powers of ξ, the following set of linear ordinary differential equations is obtained from the momentum equation:

$$\psi_0' \psi_1' - \psi_0'' \psi_1 = 0 \tag{32a}$$

$$\psi_0' \psi_2' + \psi_1'^2 - \psi_1' \psi_1'' - \psi_2 \psi_2'' = 0 \tag{32b}$$

$$\frac{1}{2}\psi_0'\psi_3' + \psi_1'\psi_2' + \frac{1}{2}\psi_2'\psi_1' - \frac{1}{2}\psi_1\psi_2'' - \psi_2\psi_1'' - \frac{1}{2}\psi_3\psi_0'' = \theta_0 + \psi_0''' \tag{32c}$$

and from the energy equation the following set of algebraic equations:

$$\psi_0'\theta_1 - \psi_1\theta_0' = 0 \tag{33a}$$

$$\psi_0'\theta_2 + \psi_1'\theta_1 - \psi_1\theta_1' - \psi_2\theta_0' = 0 \tag{33b}$$

$$\frac{1}{2}\psi'_0\theta_3 + \psi'_1\theta_2 + \frac{1}{2}\psi'_2\theta_1 - \frac{1}{2}\psi_1\theta'_2 - \psi_2\theta'_1 - \frac{1}{2}\psi_3\theta'_0 = \frac{1}{Pr}\theta_2'' \quad (33c)$$

The details of the solution of equations (32) and (33) can be found in Appendix D and the results are summarized below:

$$\begin{aligned} \psi_1 &= 0 \\ \psi_2 &= \frac{C_1}{2a_2}\psi'_0 \\ \psi_3 &= 6\psi_0 - 2y^*\psi'_0 + \frac{D_2}{2a_2}\psi'_0 \end{aligned} \quad (34)$$

$$\begin{aligned} \theta_1 &= 0 \\ \theta_2 &= \frac{C_1}{2a_2}\theta'_0 \\ \theta_3 &= (\frac{D_2}{2a_2} - 2y^*)\theta'_0 \end{aligned} \quad (35)$$

With these coefficient functions determined, velocity and temperature profiles for large y^* can be generated according to the following expansions:

$$u^* = \frac{\partial\psi}{\partial y^*} = F'(y^*) + [\frac{C_1}{4a_2}F''(y^*)]\xi^2 + [\frac{2}{3}F'(y^*) + \frac{1}{6}(\frac{D_2}{2a_2} - 2y^*)F''(y^*)]\xi^3 \quad (36)$$

and

$$\theta = H(y^*) + \frac{C_1}{4a_2}H'(y^*)\xi^2 + \frac{1}{6}(\frac{D_2}{2a_2} - 2y^*)H'(y^*)\xi^3 \quad (37)$$

D. NUMERICAL SOLUTION OF UNIVERSAL EQUATIONS

The universal equations (23)-(26) with boundary conditions (27) and (28) were solved numerically with an IBM 3033 series digital computer. Double precision machine arithmetic was used for all computations. A least squares correction method

developed by Nachsteim and Swigert [20] was used as shooting point routine to determine the unknown starting values for each set of fifth order two point boundary value equations. A standard fourth order Runge-Kutta initial value integration routine was employed to tabulate values for the free convection functions F, F', F'', H and H'; the zeroth order inner series coefficient functions f_o, f_o', f_o'', g_o and g_o'; and the higher order universal functions Y_{10}, Y_{11}, Y_{20}, etc. These tabulated values were then used to generate the inner and outer velocity and temperature profiles as well as the local Nusselt number at the surface of the plate.

IV. RESULTS

A. PRESENTATION OF RESULTS

1. Velocity and Temperature Profiles

a. Inner Series Profiles

The inner series expansions for velocity and temperature were computed form the tabulated values of the universal functions which were obtained form the numerical solution of the fifth order ordinary differential equations defined by equations (23) through (25). The velocity profiles were obtained for specified values of ε^* the blowing or suction parameter according to the following equation:

$$u^* = \xi[f'_0 + (Y'_{10} + \varepsilon^* Y'_{11})\xi + (Y'_{20} + \varepsilon^* Y'_{21} + \varepsilon^{*2} Y'_{22})\xi^2] \quad (38)$$

where the f'_0, Y'_{10}, Y'_{11}, etc., are functions of η. In order to facilitate comparison and matching of the inner and outer profiles the nondimensional velocity u^* was plotted as a function of y^* where the relationship between y^* and η is: $y^*=\xi \cdot \eta$. Numerous sets of profiles were generated for analysis and comparison; however, only the profiles corresponding to the following parameters are presented in this paper:

1) Blowing and suction parameter, ε^*, of magnitudes ± 0.05 and ± 0.25 where positive values correspond to suction and negative values to blowing.
2) Streamwise nondimensional parameter, ξ, corresponding to $\bar{x}/L$ ratios of .25, .50, and 1.0.

The plots of u* versus y* for these parameters are presented in Figures 2-13 and for ease of comparison both inner and outer profiles are included on the same plot.

The temperature profiles generated by the inner series expansions were obtained from the following equation:

$$\theta = 1 + \xi[g_0 + (Z_{10} + \varepsilon^* Z_{11})\xi + (Z_{20} + \varepsilon^* Z_{21} + \varepsilon^{*2} Z_{22})\xi^2] \tag{39}$$

where the g_0, Z_{10}, Z_{11}, etc are functions of η; however, as was the case with the velocity profiles, θ was plotted as a function of y* with $y^* = \xi \cdot \eta$. The same parameters were used in plotting θ versus y* and the outer profiles were included for comparison. These plots appear in Figures 14-25.

b. Outer Series Profiles

The outer series expansions which were constructed in the preceding chapter approximated the behavior of the velocity and temperature distributions at greater distances from the plate. The outer velocity profiles are given by equation (36) which is written below for convenience:

$$u^* = F'(y^*) + [\frac{C_1}{4a_2} F''(y^*)]\xi^2 + [\frac{2}{3}F'(y^*) + \frac{1}{6}(\frac{D_2}{2a_2} - 2y^*)F''(y^*)]\xi^3 \tag{36}$$

where F' and F'' are the first and second derivatives of the free convection stream function evaluated at the location of the discontinuity, $\bar{x} = 0$. They were numerically calculated for values of the free convection similarity variable which

is identically equal to y^* at $\bar{x} = 0$. The constant $a_2 = \frac{1}{2}F''(0)$, and the constants C_1 and D_2 are computed numerically from equations (D-16) and (D-17) respectively. The outer velocity profiles corresponding to the same ϵ^* and ξ parameters as were specified for the inner profiles are shown in Figures 2 through 13.

The outer expansion which defines the temperature profile valid for large values of y^* was given in equation (37) and is repeated below:

$$\theta = H(y^*) + \frac{C_1}{4a_2} H'^*y^*)\xi^2 + \frac{1}{6}(\frac{D_2}{2a_2} - 2y^*)H'(y^*)\xi^3 \qquad (37)$$

where the constants C_1, D_2, and a_2, are defined as before, and, the H and H' are the free convection temperature distribution and its derivative evaluated at $\bar{x} = 0$ where y^* is the free convection similarity variable. Once again the plots of θ versus y^* for the same parameters as for the inner profiles, are presented in Figures 14 through 25.

2. Heat Transfer Characteristics at the Surface

The standard method of characterising the heat transfer at the surface of a heated plate is to calculate the local Nusselt number at the point of interest. In this particular problem the Nusselt number at any location above the discontinuity, $\bar{x}>0$, is given by the following:

$$Nu = -\frac{L}{(\bar{T}_w - \bar{T}_\infty)} \frac{\partial \bar{T}}{\partial \bar{y}}\Big|_{\bar{y}=0} \qquad (40)$$

which reduces to the following form when the appropriate substitutions are made for $\bar{T}$ and $\bar{y}$ in terms of nondimensional variables:

$$Nu = -\left(\frac{Gr}{4}\right)^{\frac{1}{4}} \left[g_0'(0) + \left(Z'_{10}(0) + \varepsilon^* Z'_{11}(0)\right)\xi + \left(Z'_{20}(0) + \varepsilon^* Z'_{21}(0) + \varepsilon^{*2} Z'_{22}(0)\right)\xi^2\right] \quad (41)$$

where the universal functions Z'_{10}, Z'_{11}, etc. were numerically evaluated at $\eta = 0$. The heat transfer data is presented in graphical form using the following nondimensional parameter

$$\frac{Nu}{\left(\frac{Gr}{4}\right)^{\frac{1}{4}}}$$

which was plotted as a function of ξ for the following values of the suction and blowing parameter:

$\varepsilon^* = \pm 0.05$ and ± 0.25.

The results are presented in Figures 26-29.

B. DISCUSSION OF RESULTS

1. The Matching Condition

a. The End-Point of Numerical Integration.

The end-point of numerical integration is the value supplied to the Nachsteim and Swigert starting value routine at which it attempts to satisfy the boundary conditions at $\eta = \infty$. The choice of this point has an obvious direct influence on the starting values, $f_k''(0)$ and $g_k'(0)$, and also on the outer series constants C_{10}, C_{11}, D_{20}, D_{21} and D_{22} defined in (C-16) and (C-17) and which were numerically evaluated at

the value of η chosen as the end-point. A summary of the effects of varying the end-point on both the starting values and outer series constants is presented in Table I. For each of the end-point values, η_{end}, listed in the table, a complete set of tabular profiles were generated and qualitatively compared to determine the degree of matching evidenced. The results of this process revealed that the smaller the value of η_{end}, the better was the overall matching of the profiles. However, for η_{end} <2.0 no further improvement in the matching was observed. Also, the boundary conditions at $\eta = \infty$ were satisfied to equal degrees of accuracy for each η_{end} selected. Therefore, all of the numerical results presented were based on an end-point value of $\eta_{end} = 2.0$. It was also observed that the outer profiles were quite insensitive to variations in the constants C_{10}, C_{11}, etc,; and that for a fixed ε^* and ξ the parameter $Nu(Gr/4)^{-1/4}$ was insensitive to changes in the initial values which were caused by changing η_{end}.

b. The Inner-Outer Profile Match Point

In addition to the qualitative numerical procedure outlined above to effect a matching of the inner and outer profiles, another approach was undertaken based on the application of an overall energy balance to the problem under consideration. The principle of conservation of energy requires that all energy entering a specified control volume must leave that volume providing there is no storage of energy within the volume. In the case of the present problem all of the energy

TABLE I

SUMMARY OF STARTING VALUES AND MATCHING CONSTANTS

η_{end}	2.0	3.0	5.0	7.0	10.0
$Y''_{10}(0)$	10^{-9}	10^{-9}	10^{-9}	0	0
$Z''_{10}(0)$	10^{-9}	10^{-9}	10^{-9}	0	0
$Y''_{11}(0)$	2.5787	2.8611	3.0893	3.1745	3.2263
$Z'_{11}(0)$	-1.5531	-1.7623	-1.9329	-1.9994	-2.0403
$Y''_{20}(0)$	10^{-4}	10^{-4}	10^{-4}	10^{-5}	10^{-10}
$Z'_{20}(0)$	10^{-4}	10^{-4}	10^{-5}	10^{-5}	10^{-8}
$Y''_{21}(0)$	-2.5437	-3.3282	-4.0277	-4.3080	-4.4860
$Z'_{21}(0)$	.12905	.21959	.345070	.4034	.44235
$Y''_{22}(0)$	2.15407	2.3655	2.7645	2.9743	3.1229
$Z'_{22}(0)$	-.96015	-.9905	-1.18464	-1.3222	-1.4087
C_{10}	0	0	0	0	0
C_{11}	1.605	1.636	1.622	1.615	1.61
D_{20}	0	0	0	0	0
D_{21}	3.2534	4.403	7.022	9.875	14.289
D_{22}	-2.8477	-2.9755	-2.9811	-2.8945	-2.788

entering the system at the surface of the plate must exit in an upward direction parallel to the plate. The mathematical formulation of this requirement is presented below in integral form.

$$\int_0^\infty c_p \rho (\bar{T} - \bar{T}_\infty) \bar{u} d\bar{y} = \int_0^{\bar{x}+L} q''(\bar{x}) d\bar{x} \qquad (42)$$

The left hand integral must be divided into two separate integrals since there exists an inner and outer region where the velocity and temperature behavior are described by different expansions--the inner and outer profiles. The dividing line between these two regions must, therefore, define the match point of the inner and outer profiles. The details of evaluating the integral equation (42) are presented in Appendix E. The only quantative result of the energy balance analysis was that an exact balance could be achieved only if the matching point between the inner and outer expansions is taken to be $y^* = 0$. That is the integral in (42) must be evaluated using the outer series to account for energy leaving the volume---the left side--and the inner series to account for the thermal energy entering the volume at the surface of the plate. As the profiles themselves suggest, the outer profiles when viewed in an integrated or global sense more nearly satisfy the energy balance, although in a pointwise sense they clearly do not, especially at the surface of the plate. Since behavior at the surface of the plate whether with respect to heat transfer or shear stress is of primary interest, from

an engineering standpoint, knowledge of the exact location of the match point is not essential, since the inner series expansions are always used to furnish results at the surface.

2. Velocity Profiles

Before analyzing the velocity profiles some method of characterizing the relative magnitude of the blowing or suction velocity should be established. To accomplish this $\bar{v}_w$ will be compared to the maximum value of the u-component of velocity in the case of unperturbed free convection evaluated at the location of the discontinuity, $\bar{x} = 0$, which will be designated by $\bar{u}_{max}$. The ratio $\bar{v}_w/\bar{u}_{max}$ which characterises this comparison is reduced to the following nondimensional form through appropriate substitutions:

$$\frac{\bar{v}_w}{\bar{u}_{max}} = 5.124\ \varepsilon^* Gr^{\frac{1}{4}} \tag{43}$$

For a $Gr \approx 10^8$ for which the laminar flow regime is still applicable the relationship expressed in (43) becomes:

$$\frac{\bar{v}_w}{\bar{u}_{max}} = .0512\ \varepsilon^* \tag{44}$$

From this correlation the blowing and suction parameters used in the present problem correspond to the following specific relationships:

$$\varepsilon^* = 0.05 \quad \text{implies} \quad \bar{v}_w = .00256\ \bar{u}_{max},$$
$$\text{and} \tag{45}$$
$$\varepsilon^* = 0.25 \quad \text{implies} \quad \bar{v}_w = .0128\ \bar{u}_{max}$$

These values for $\bar{v}_w$ are consistent with the original assumption underlying the governing boundary layer equations.

A careful review of the inner profiles plotted in Figures 2-13 reveals the following features about velocity behavior with suction or blowing:

1) As suction is increased at a specified value of $\frac{\bar{x}}{L}$, the location of the maximum u* is drawn in closer to the plate and its magnitude is decreased.
2) At a given value of suction the location of the maximum u* is moved closer to the plate and the magnitude of u* is decreased as the value of $\frac{\bar{x}}{L}$ is increased.
3) The results for blowing exhibit the reverse effects on the location and magnitude of u* as those described in 1) and 2) for suction.

Numerical data on the effects of suction and blowing on the location and magnitude of the maximum u* for the inner velocity profiles as well the corresponding data for the unperturbed free convection case is presented in Table II.

Comparison of the suction data with the free convection data reveals that the location of the maximum u* is shifted closer to the plate and also that its magnitude is reduced by 15% when $\frac{\bar{x}}{L}$ =0.25 and by 37% when $\frac{\bar{x}}{L}$ = 1.0 with a suction magnitude of ε^* =0.05. When the suction is increased to ε^*=0.25 the effects are correspondingly amplified. Although this is

TABLE II

LOCATION OF INNER PROFILE MAXIMUM VELOCITIES

	$\frac{x}{L}$ = .25	.50	1.0
Free Convection:			
y^*	1.020	1.070	1.15
u^*_{max}	.3088	.3383	.3907
Suction ε^*=0.05			
y^*	.8356	.8221	.7814
u^*_{max}	.2623	.2568	.2444
Suction ε^*=0.25			
y^*	.6868	.6634	.4906
u^*_{max}	.2426	.2194	.1862
Blowing ε^*=-0.05			
y^*	.8929	.9086	.9267
u^*_{max}	.2665	.2717	.2851
Blowing ε^*=-0.25			
y^*	.9780	.9951	1.036
u^*_{max}	.2589	.2745	.3333

the behavior which would be expected for suction, the percent reduction in maximum velocity predicted by the inner expansion is probably too great considering the relative magnitude of suction applied. In the case of blowing the inner series fails to produce results consistent with expected physical behavior since neither the location of the maximum u* is moved farther from the plate nor is the magnitude of u* increased above that observed for free convection. Also the degree of matching between the inner and outer profiles lessens as the suction magnitude or distance from the discontinuity is increased.

As indicated above the results obtained in the case of suction are consistent with the physical situation since in this case heated fluid is drawn closer to the plate where viscous forces tend to reduce the maximum velocity in the streamwise direction. In the case of blowing heated fluid is pushed farther from the surface away from the influence of viscous forces and into the region where buoyancy forces act to accelerate the flow in the streamwise direction thereby increasing the maximum u*. In addition for a specific value of either suction or blowing the effects described above will be accentuated as the distance from the discontinuity is increased; i.e.; for increasing values of $\frac{\overline{x}}{L}$ or ξ, since the blowing or suction effects will have had a greater opportunity to predominate over unperturbed free convection.

The lack of positive correlation in the case of blowing versus unperturbed free convection might be attributed to any of the following:

1) Insufficient terms in the inner series expansion; since the signs of the coefficient functions alternate in a pairwise manner, addition of another term would possible serve to effect a better correlation.
2) The effects of blowing become significant in the region where the inner series no longer provides a valid representation of the velocity behavior.

The effects of suction and blowing on the outer velocity profiles are graphically presented in Figures 2-13; however, the specific effects on the location and magnitude of the maximum value of u* are given in Table III using the same format as Table II for the inner profiles. The results in the case of suction are somewhat inconsistent with the behavior expected relative to the free convection case. The location of the maximum velocity does not move closer to the plate, and its magnitude does not decrease when compared to the free convection profiles. This anomaly suggests that the effects of suction on velocity are more significant in the region close to the surface of the plate where the behavior is better approximated by the inner series expansion. Conversely, in the blowing case the results correlate well with expected

TABLE III

LOCATION OF OUTER PROFILE MAXIMUM VELOCITIES

	$\frac{x}{L}$: .25	.50	1.0
Free Convection:			
y^*	1.020	1.070	1.150
u^*_{max}	.3088	.3383	.3907
Suction ε^*=0.05			
y^*	1.053	1.1588	1.3628
u^*_{max}	.3110	.3466	.4212
Suction ε^*=0.25			
y^*	.9386	.9519	1.1072
u^*_{max}	.3117	.3468	.4160
Blowing ε^*=-0.05			
y^*	1.110	1.240	1.472
u^*_{max}	.312	.350	.433
Blowing ε^*=-0.25			
y^*	1.206	1.370	1.617
u^*_{max}	.317	.364	.466

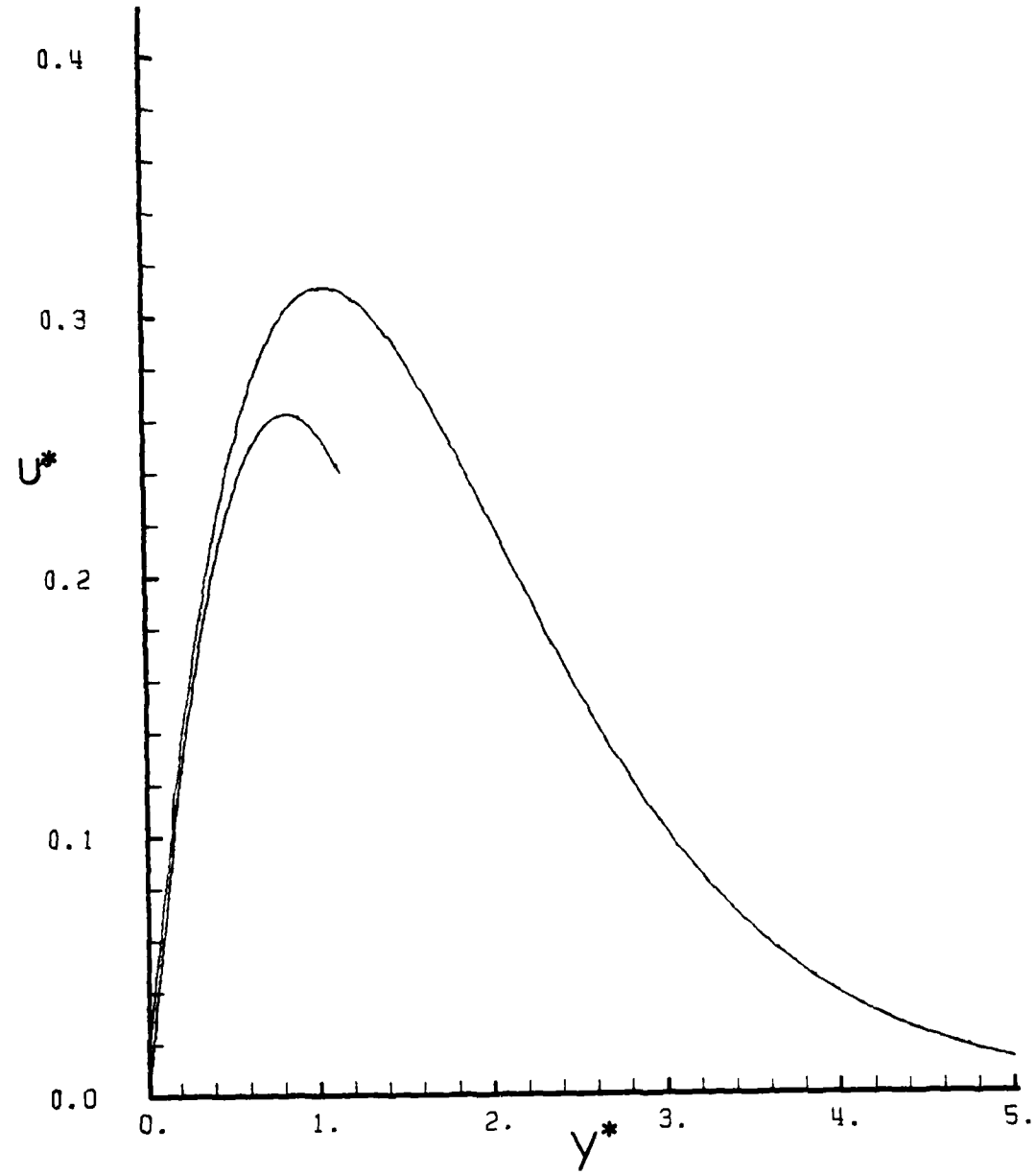

Figure 2. Suction Velocity Profiles: $\epsilon^* = 0.05$, $\frac{\bar{x}}{L} = 0.25$

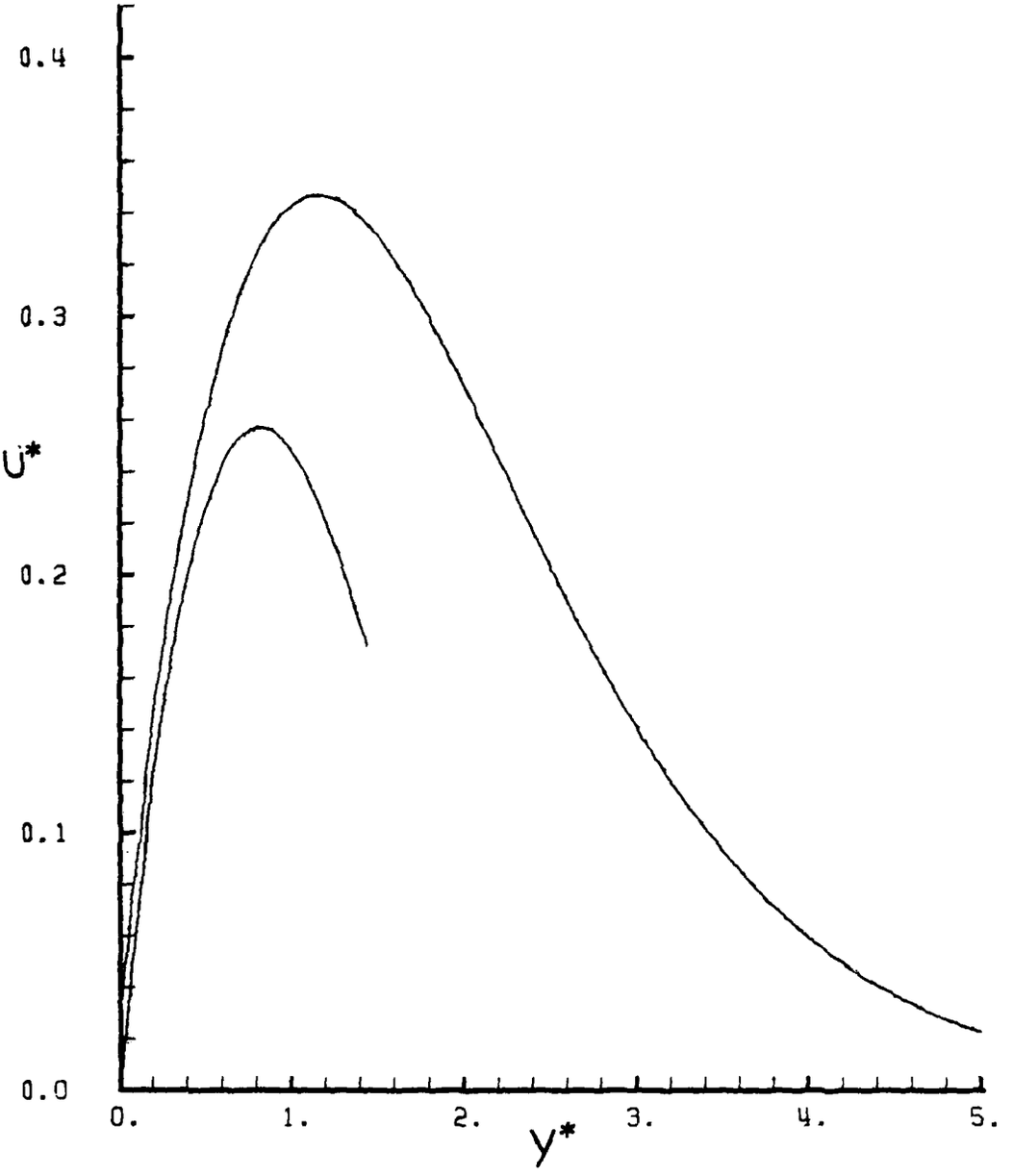

Figure 3. Suction Velocity Profiles: $\varepsilon^* = 0.05$, $\frac{\overline{x}}{L} = 0.50$

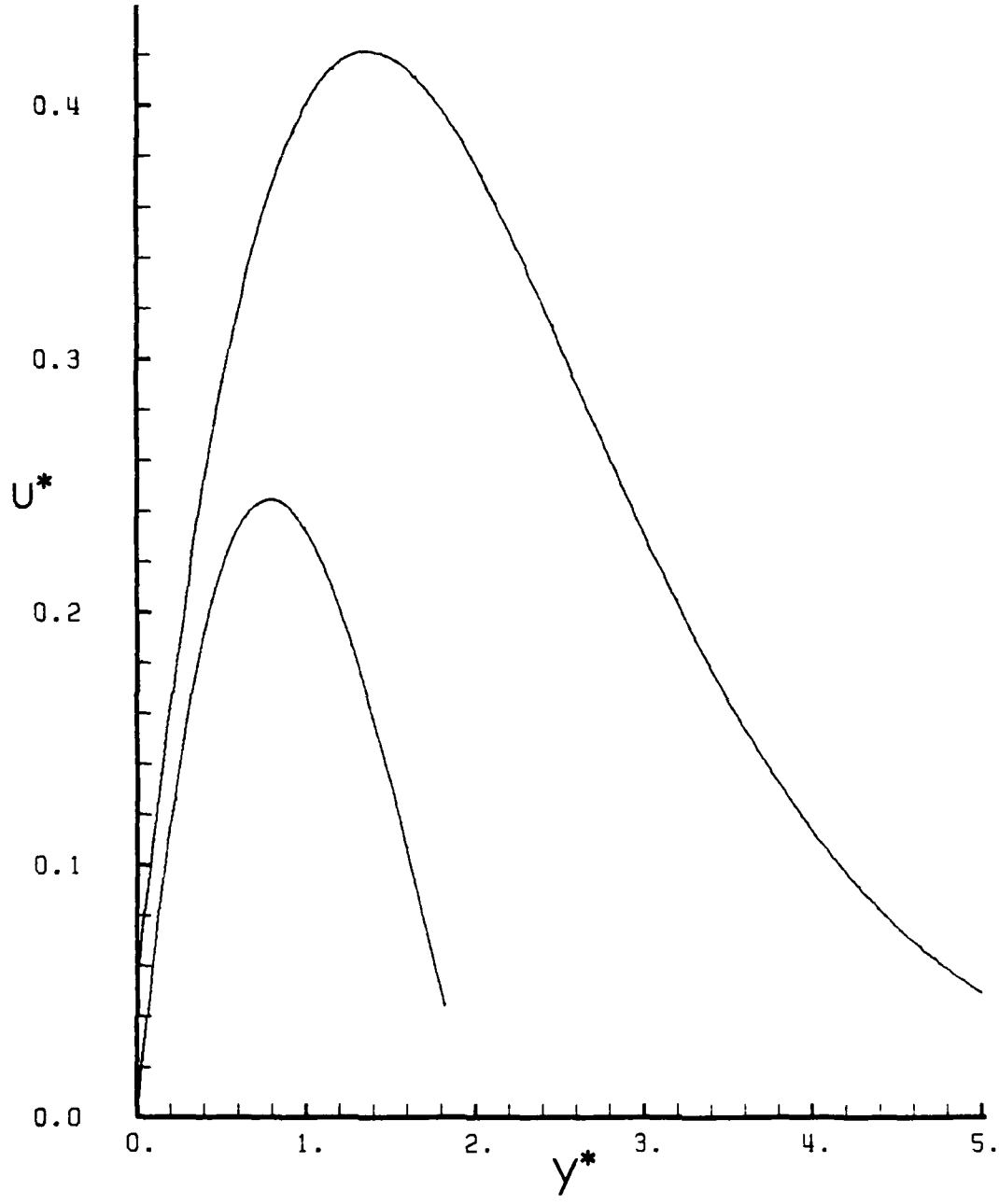

Figure 4: Suction Velocity Profiles: $\epsilon^* = 0.05$, $\frac{\bar{x}}{L} = 1.0$

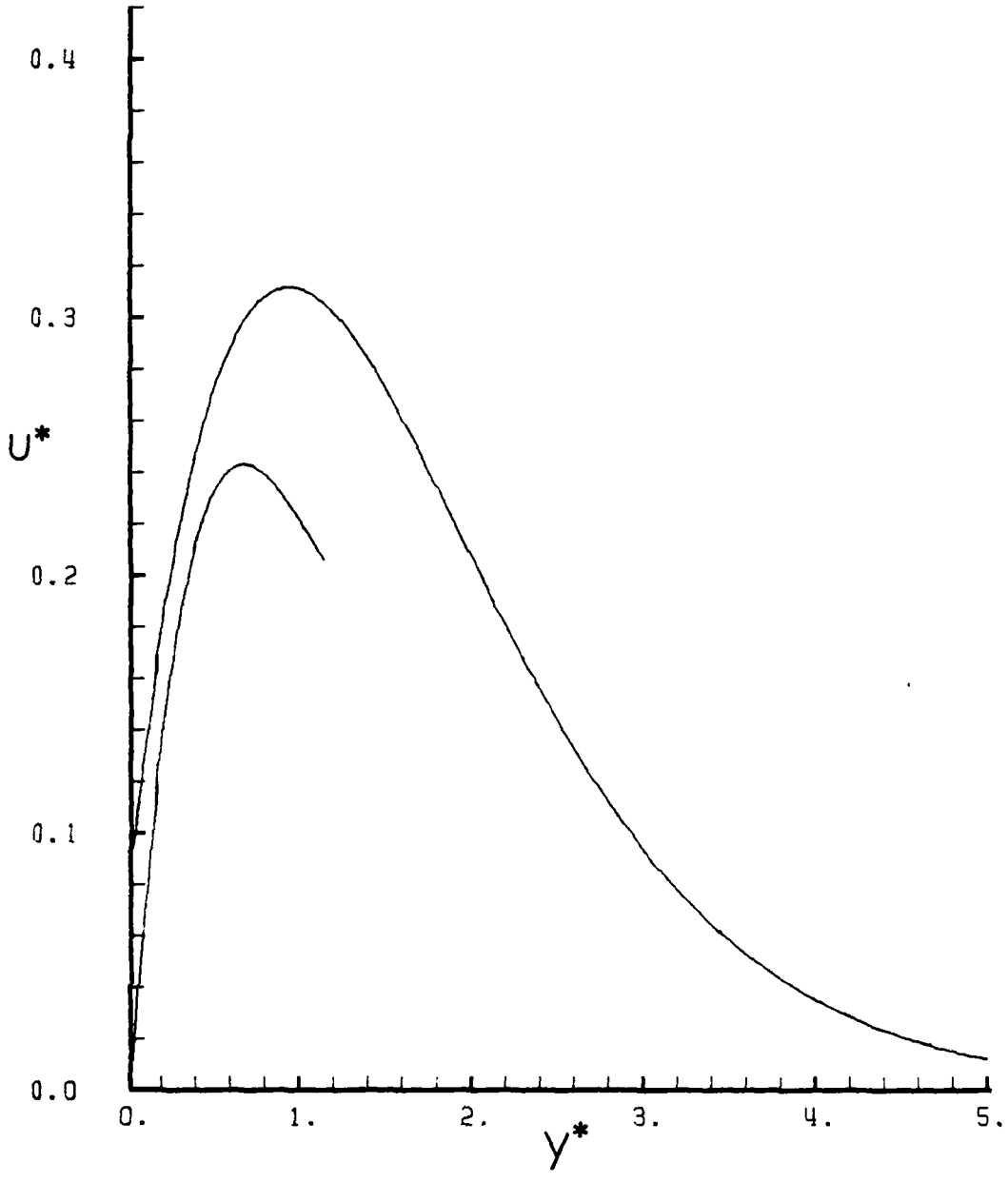

Figure 5: Suction Velocity Profiles: $\varepsilon^* = 0.25$, $\frac{\bar{x}}{L} = 0.25$

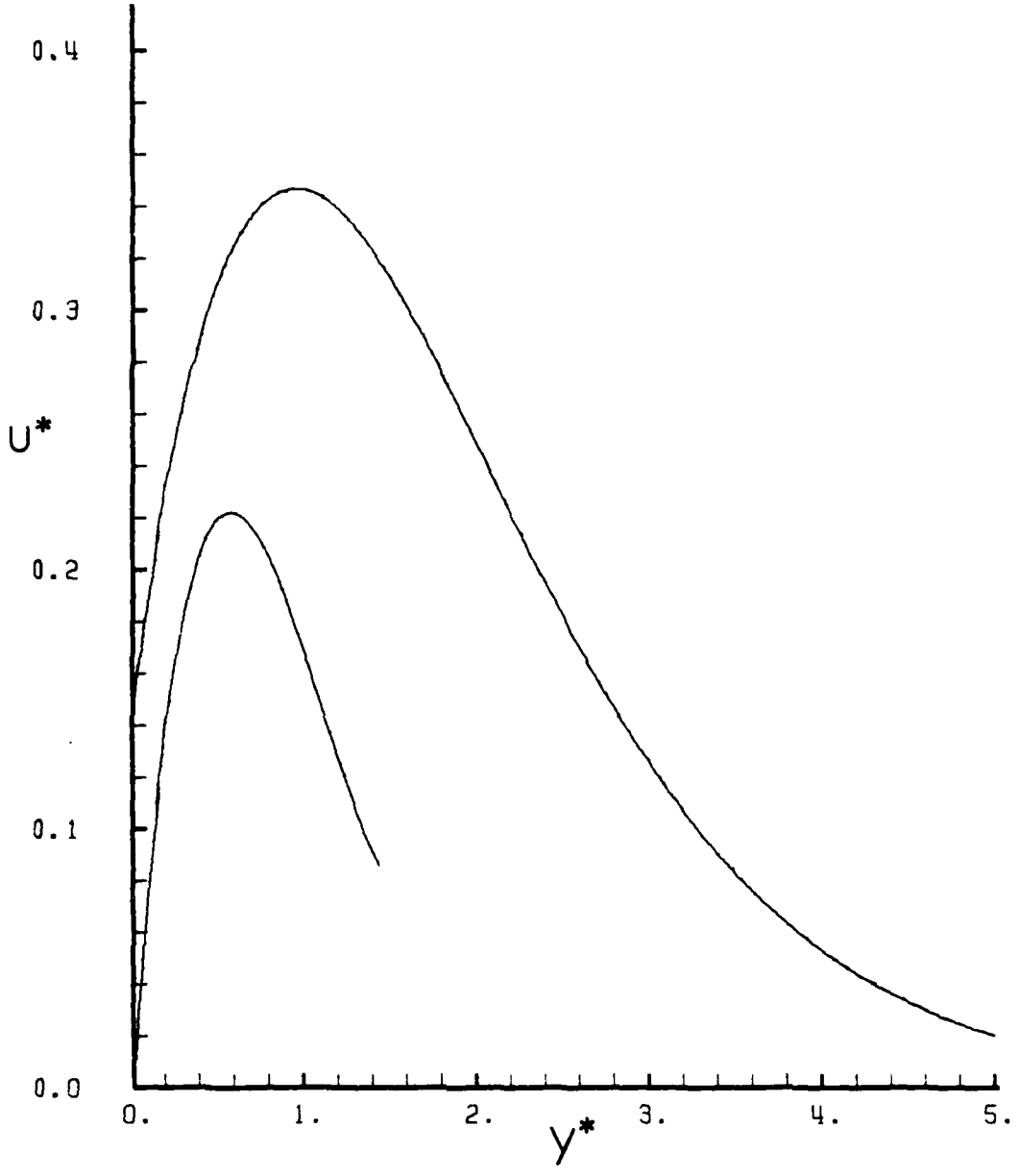

Figure 6: Suction Velocity Profiles: $\varepsilon^* = 0.25$, $\frac{\overline{x}}{L} = 0.50$

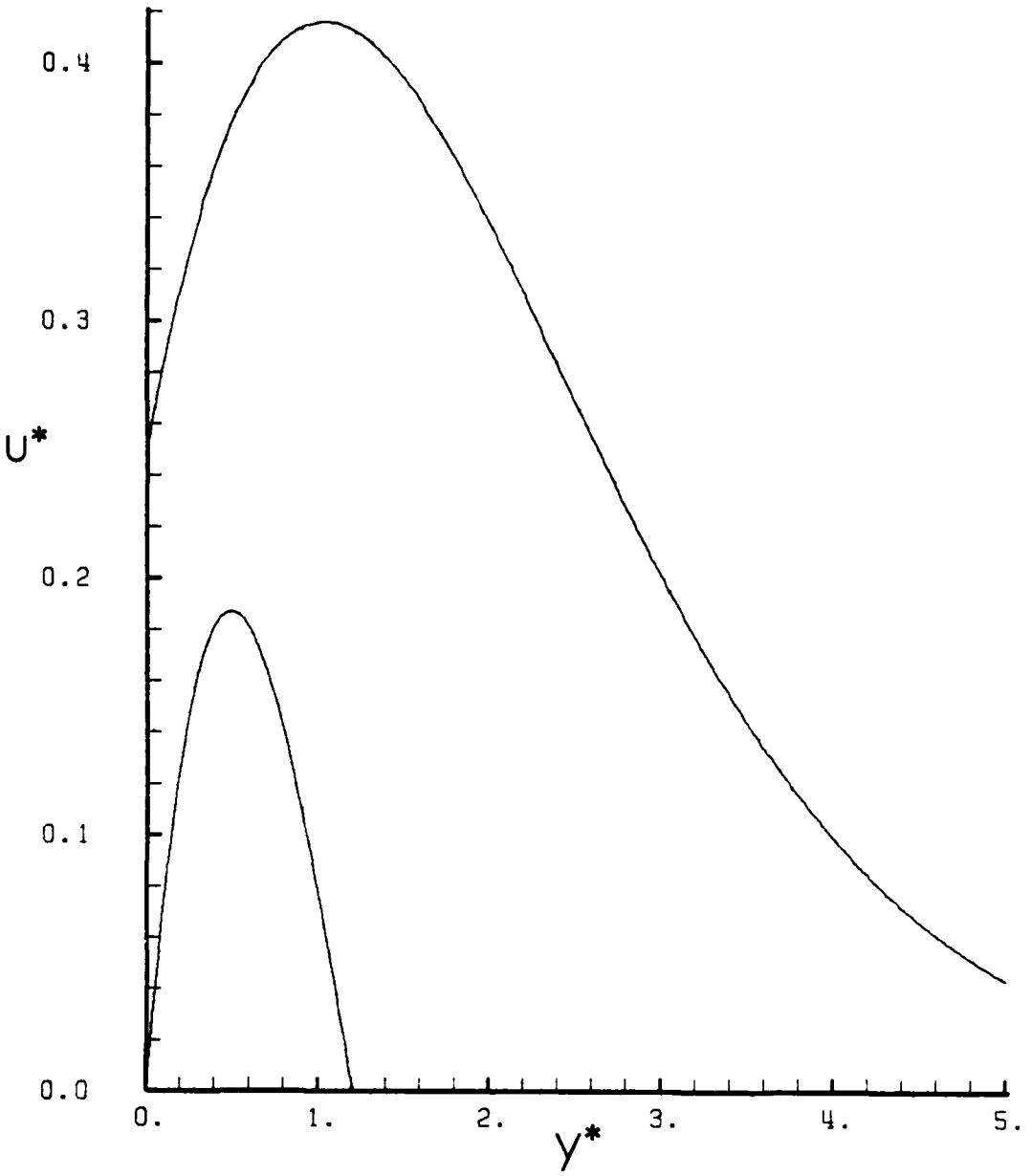

Figure 7: Suction Velocity Profiles: $\epsilon^* = 0.25$, $\frac{\overline{x}}{L} = 1.0$

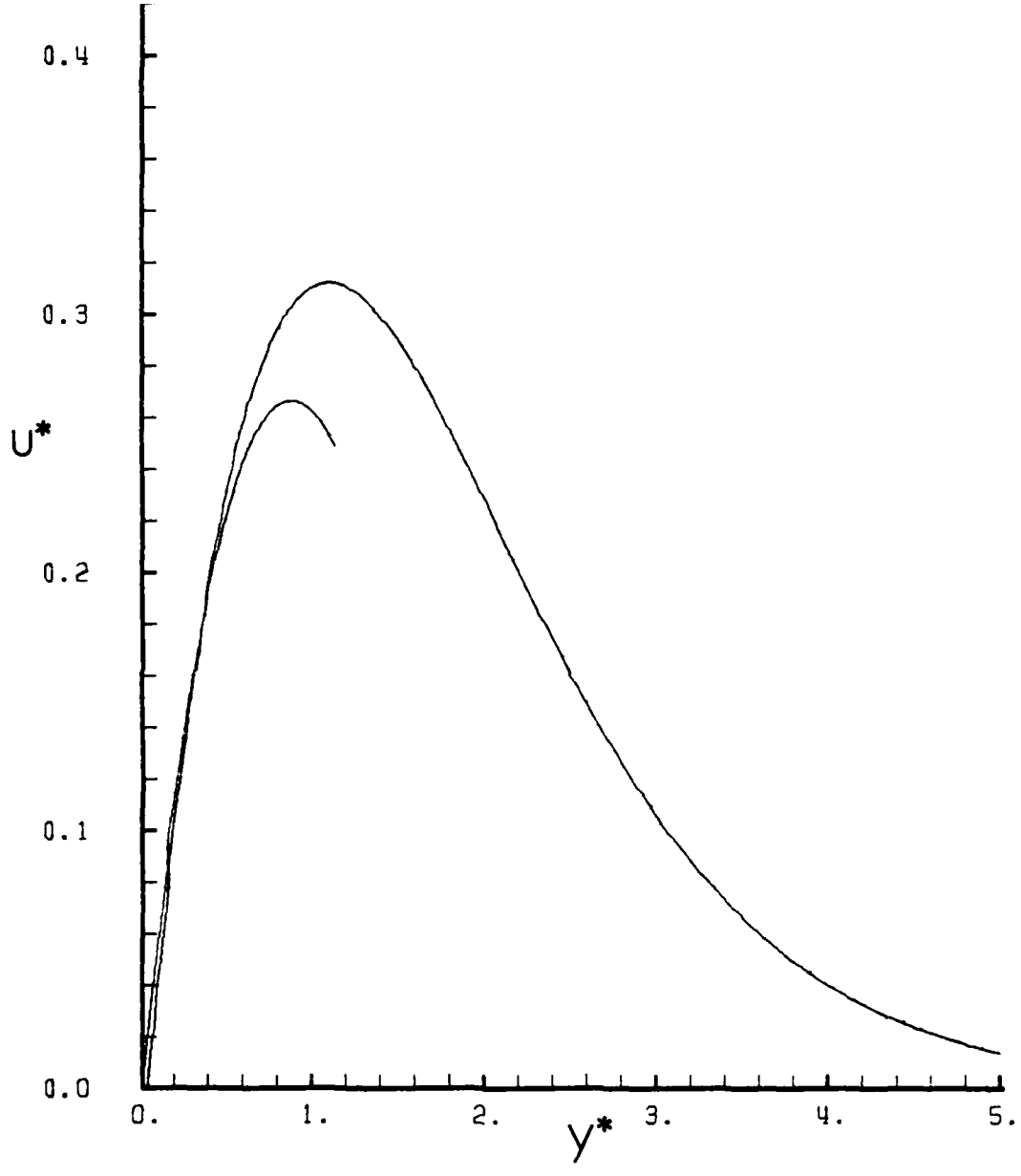

Figure 8: Blowing Velocity Profiles: $\varepsilon^* = -0.05$, $\frac{\overline{x}}{L} = 0.25$

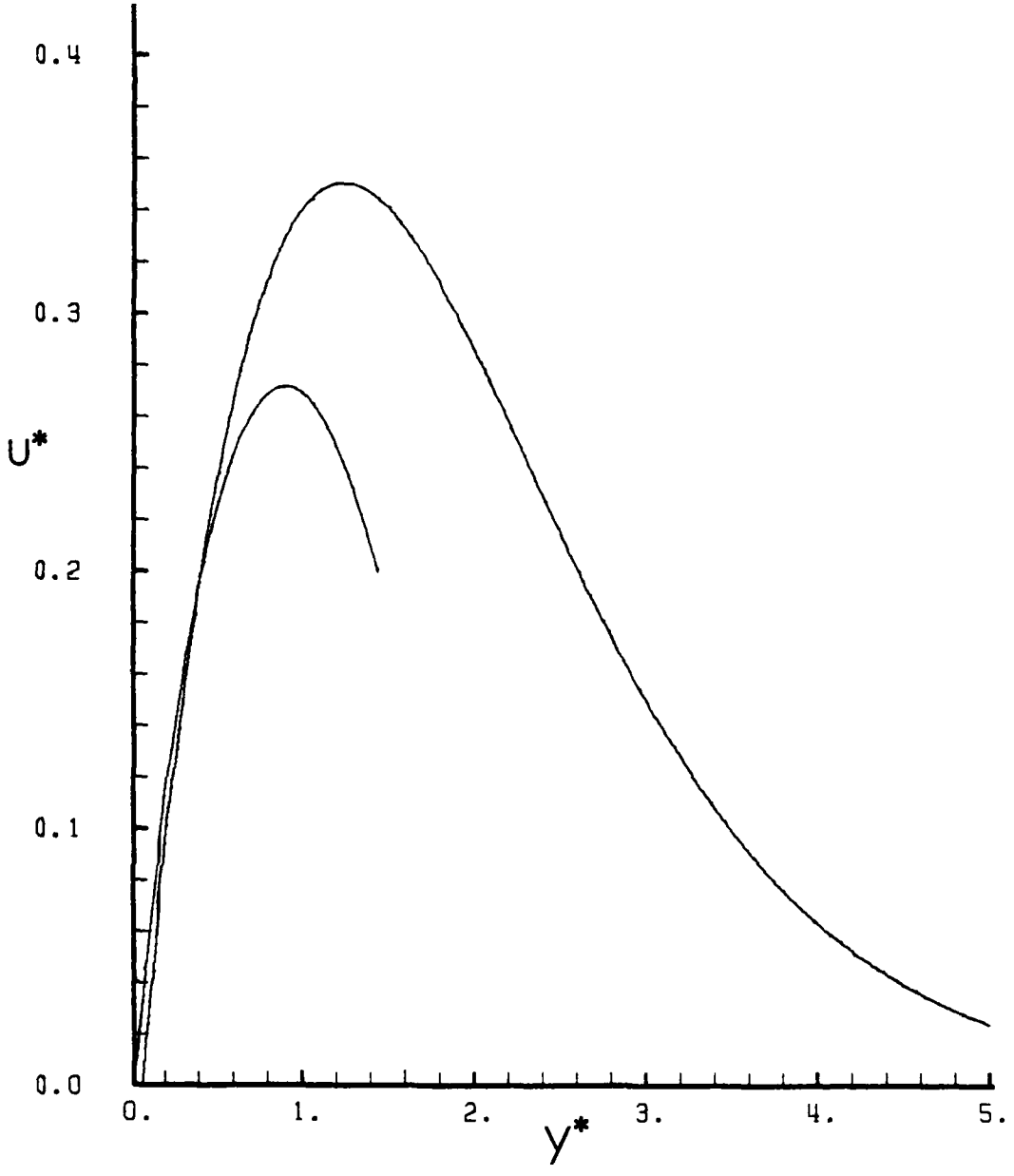

Figure 9: Blowing Velocity Profiles: $\varepsilon^* = -0.05$, $\frac{\overline{x}}{L} = 0.50$

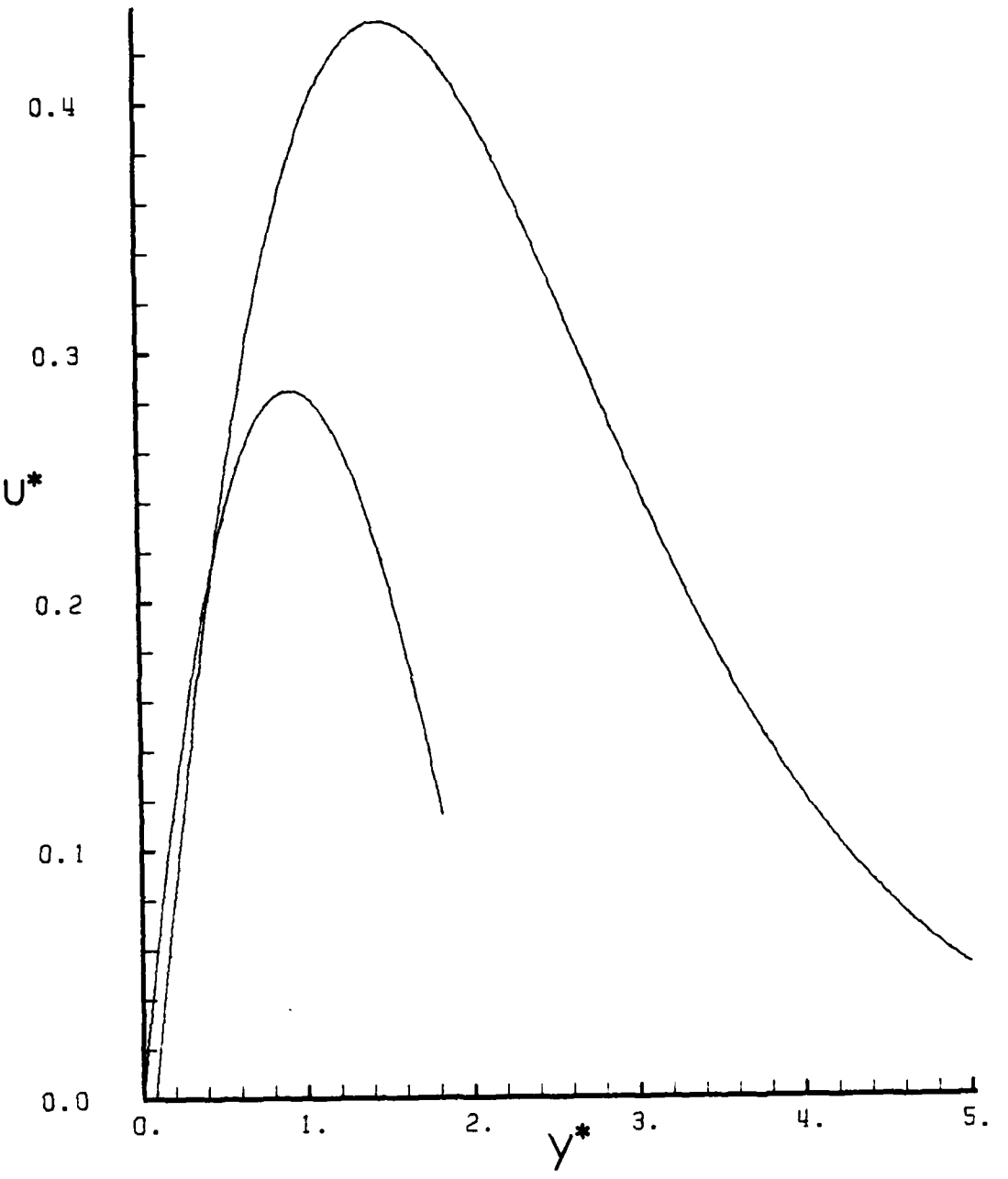

Figure 10: Blowing Velocity Profiles: $\varepsilon^* = -0.05$ $\frac{\bar{x}}{L} = 1.0$

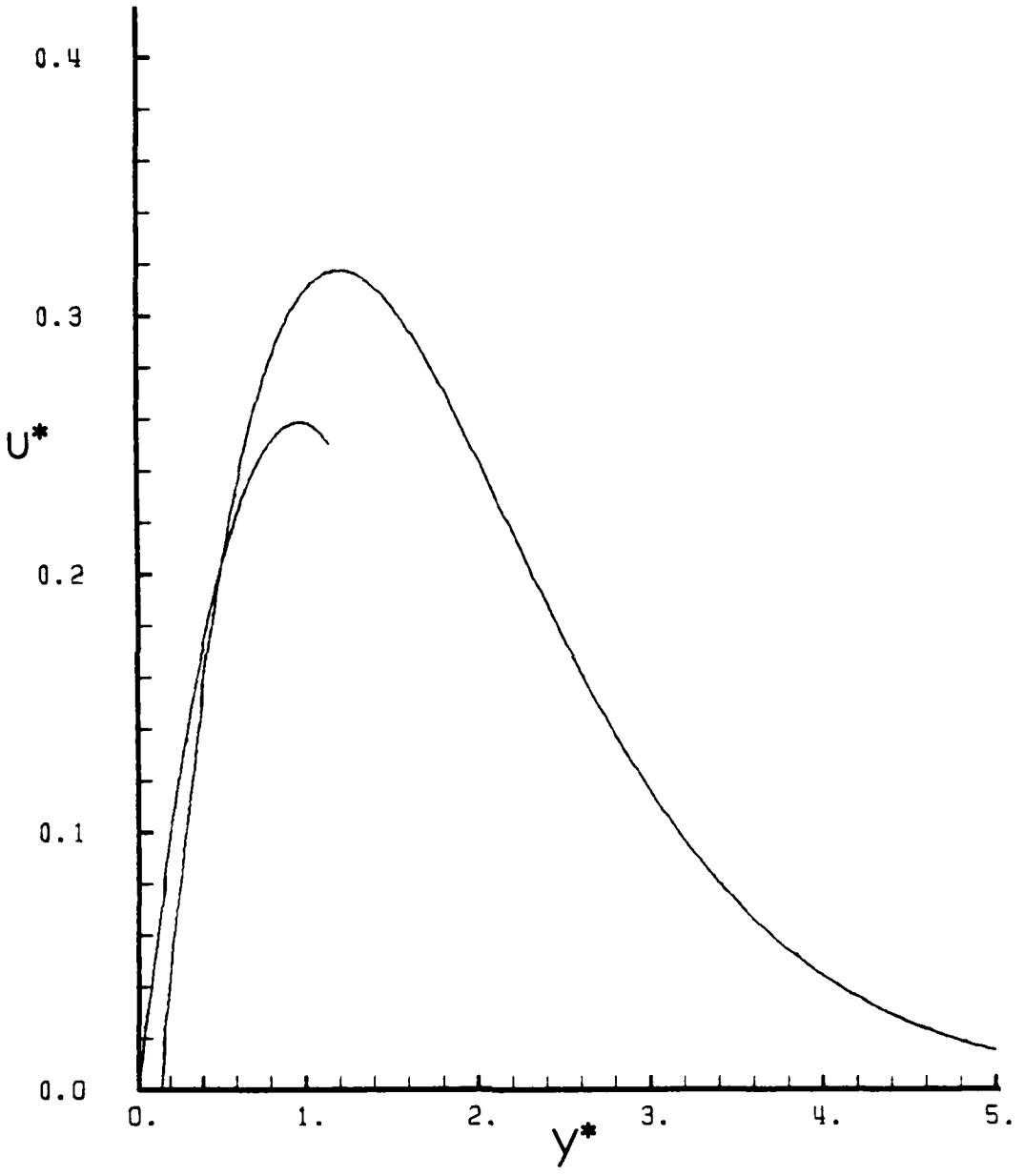

Figure 11: Blowing Velocity Profiles: $\epsilon^* = -0.25$, $\frac{\overline{x}}{L} = 0.25$

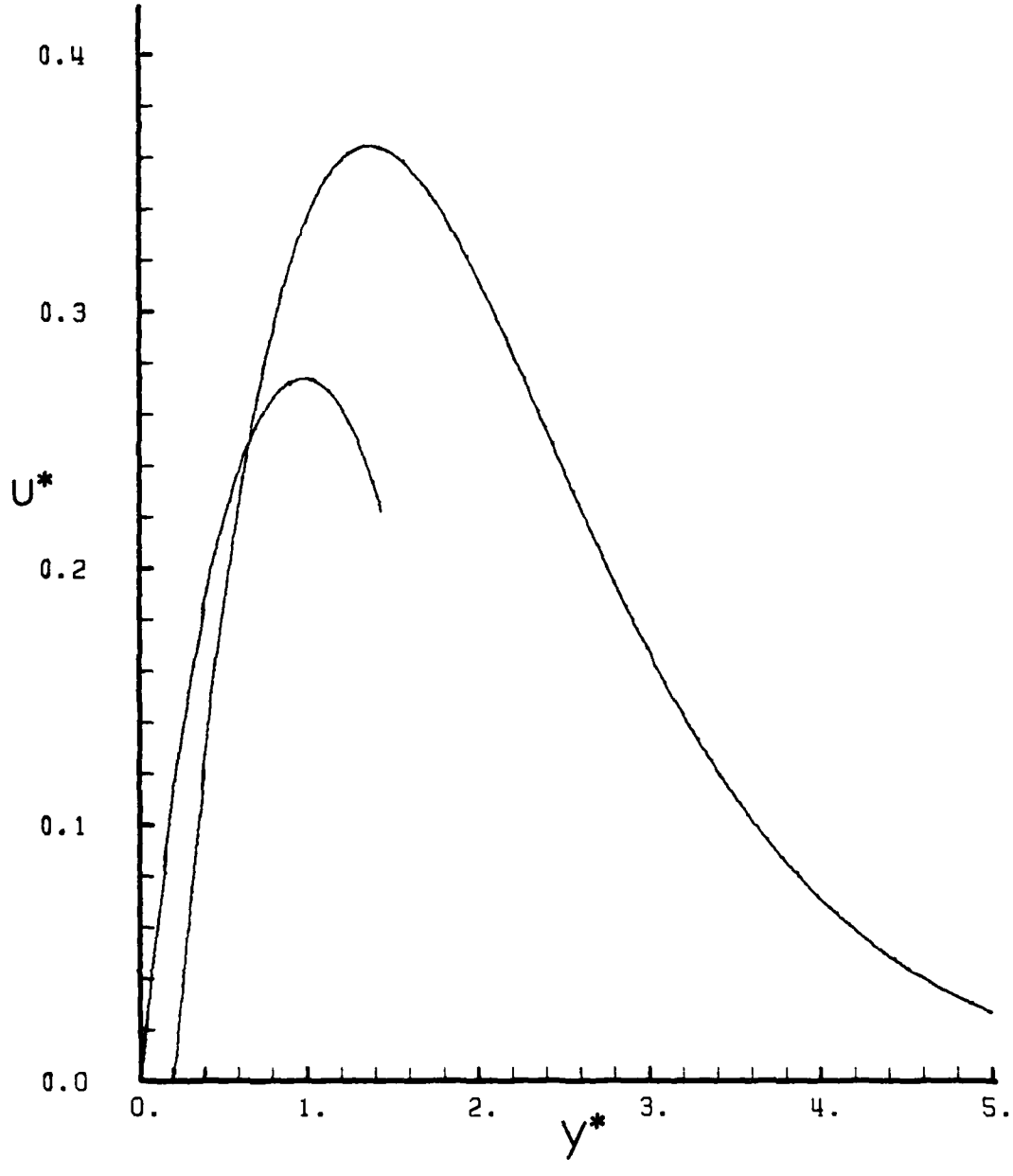

Figure 12: Blowing Velocity Profiles: $\varepsilon^* = -0.25$, $\frac{\bar{x}}{L} = 0.50$

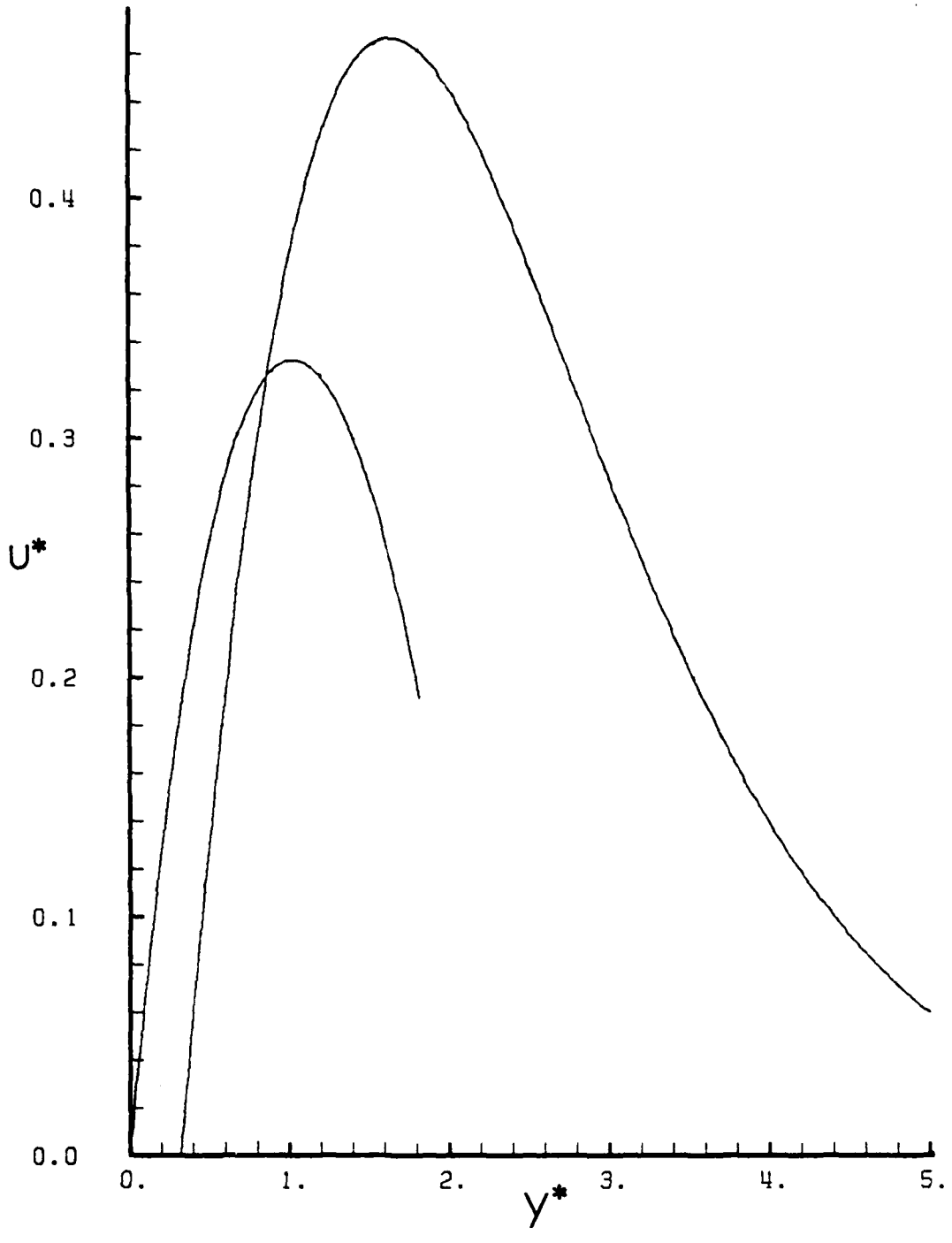

Figure 13: Blowing Velocity Profiles: $\varepsilon^* = -0.25$, $\frac{\bar{x}}{L} = 1.0$

behavior. Relative to the free convection case the maximum value of u* moves away from the plate, and its magnitude increases from 1.0% to 10.8%, with a blowing parameter $\varepsilon^*=-.05$, as $\frac{\bar{x}}{L}$ increases from .25 to 1.0. When the blowing magnitude is $\varepsilon^* = -0.25$, the value of u^*_{max} increases from 2.7% to 19.2% as $\frac{\bar{x}}{L}$ increases from .25 to 1.0. Whether or not this increase is excessive must await comparison with experimentally obtained data. In any case it appears that a very small perturbation of the momentum boundary layer at the wall, produces relatively significant changes at increased distances from the plate.

3. Temperature Profiles

The effects of blowing and suction on the temperature profiles are not as visible in the plots Figures 14-25, as was the case for velocity since there are no maximum velocity peaks to observe. However, the same general pattern emerges as did with the velocity profiles, and key points are summarized below for the inner temperature profiles:

1) For a given location above the discontinuity the inner profile pivots clockwise about $\theta = 1.0$ as the magnitude of suction is increased, this represents an increase in the gradient which is characteristic of an increased heat transfer rate.
2) For given magnitude of suction there is a marked increase in gradient as the distance from the discontinuity in the streamwise direction is increased, i.e., the value of $\frac{\bar{x}}{L}$ increases.

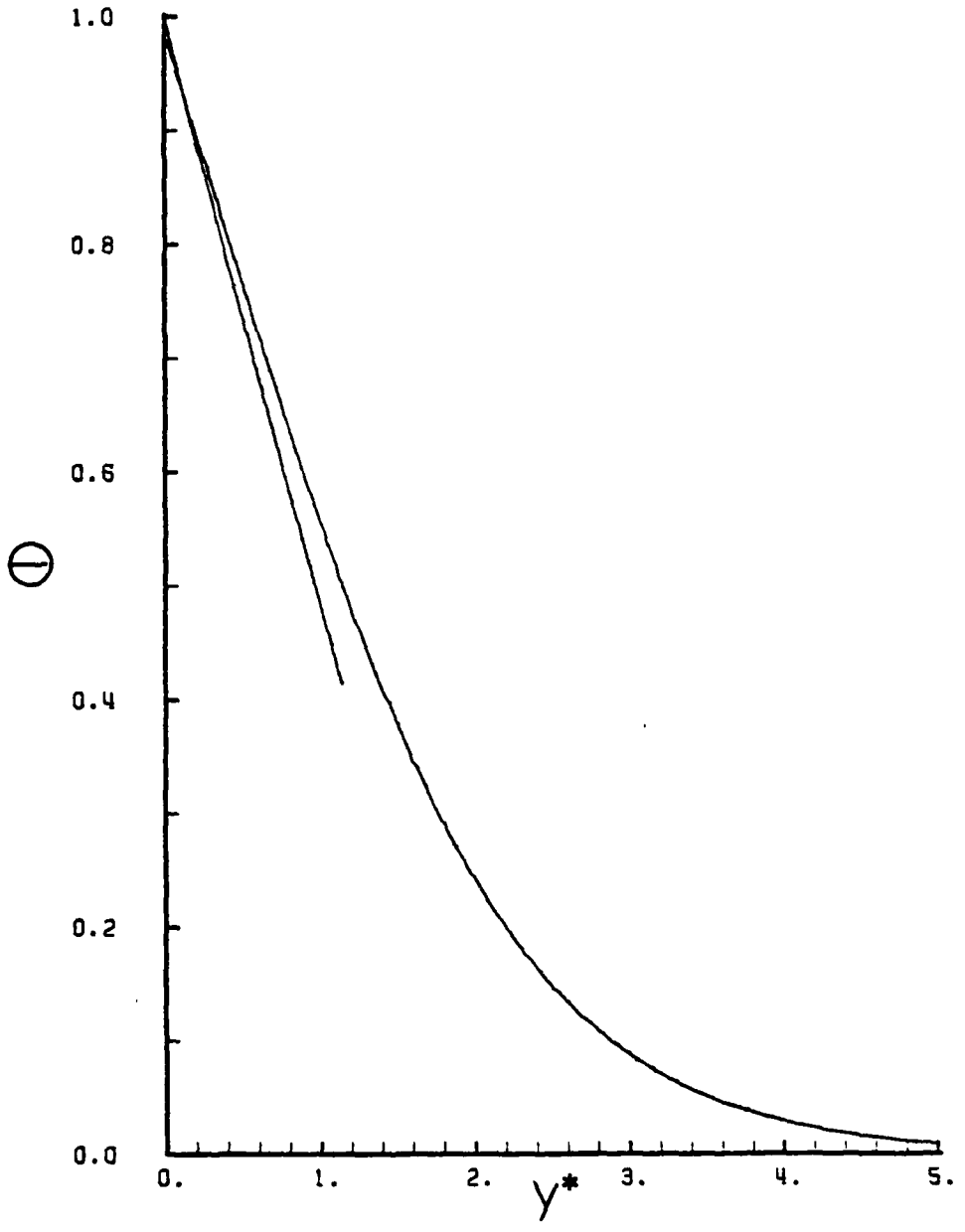

Figure 14: Suction Temperature Profiles: $\varepsilon^* = 0.05$, $\frac{\overline{x}}{L} = 0.25$

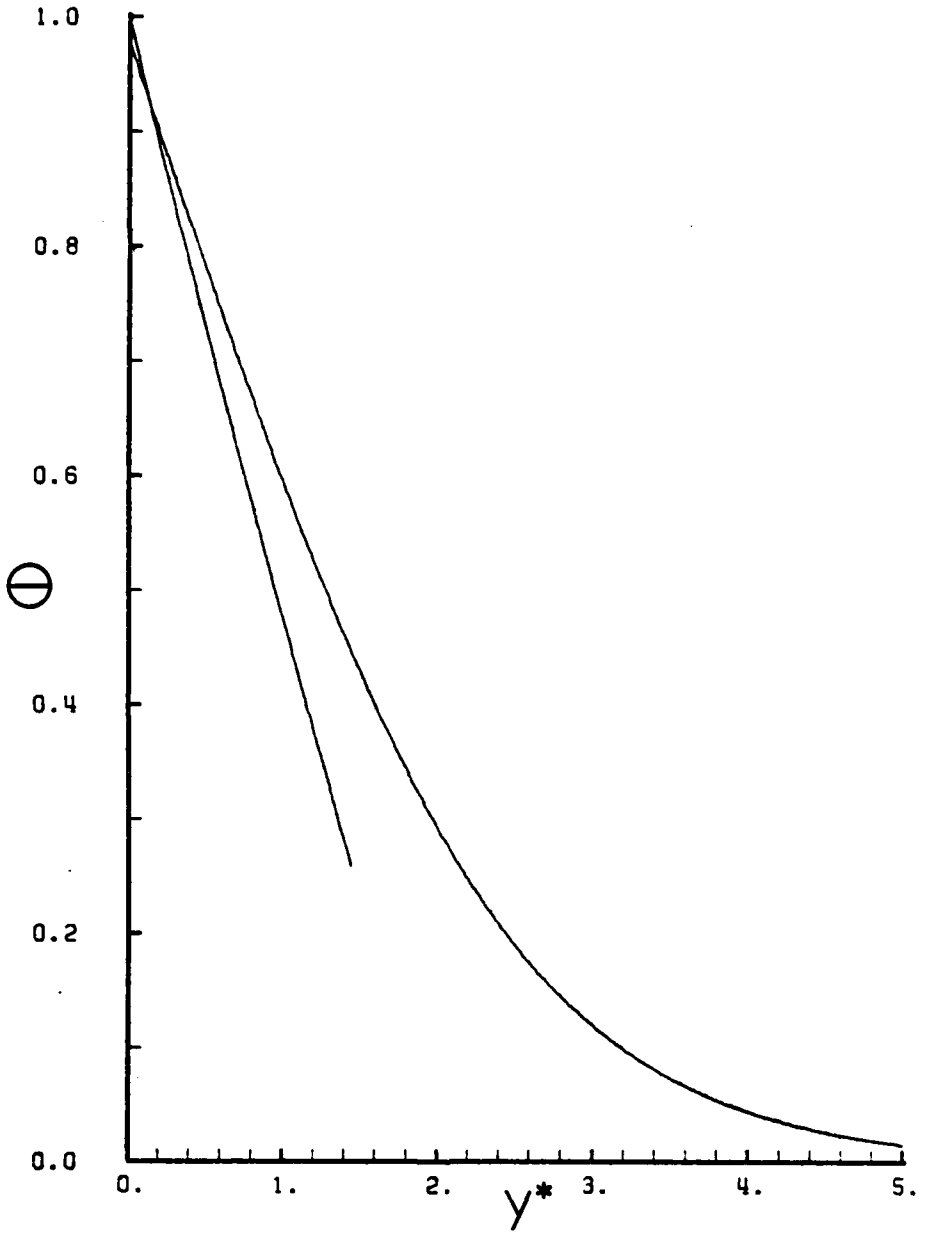

Figure 15: Suction Temperature Profiles: $\varepsilon^* = 0.05$, $\frac{\bar{x}}{L} = 0.50$

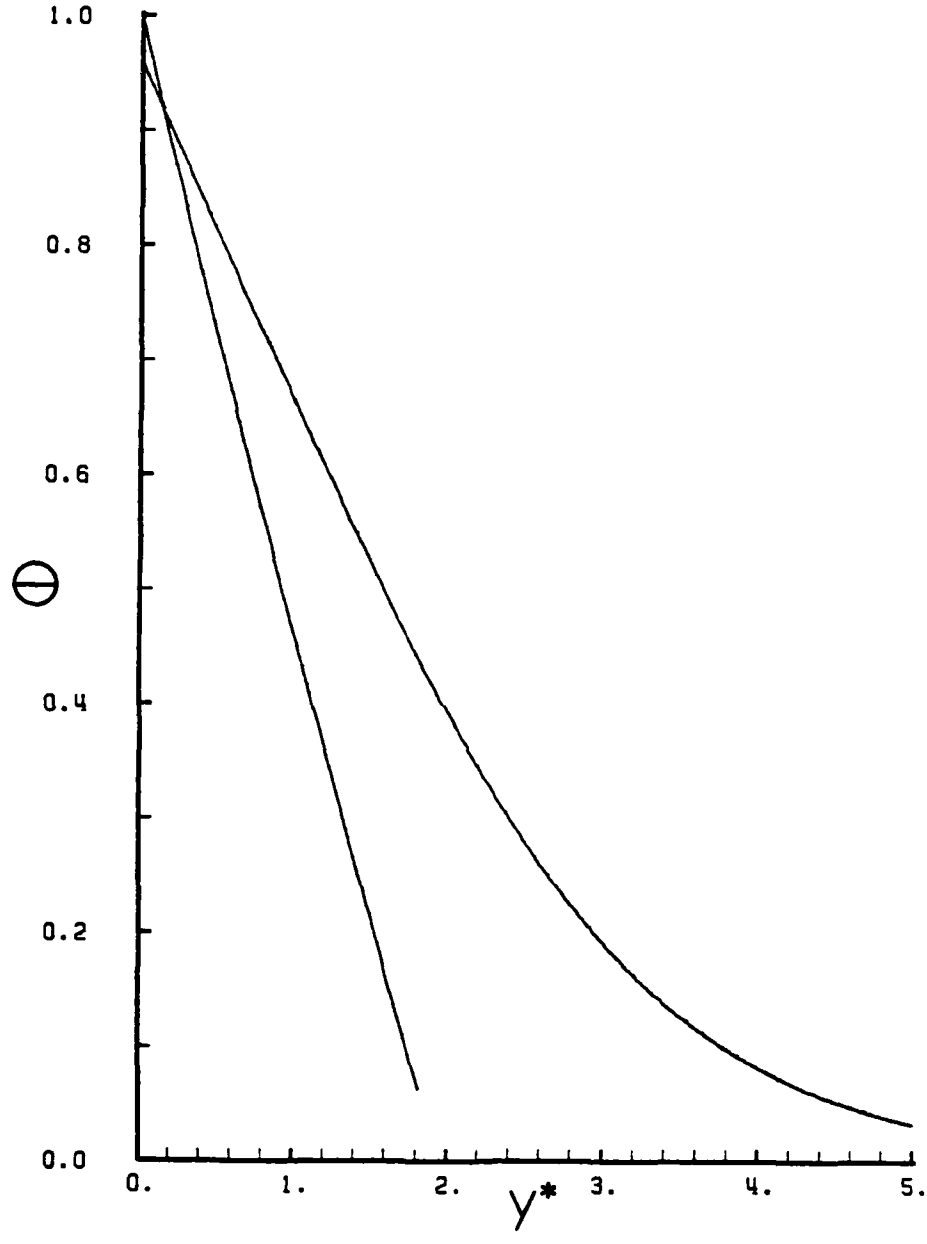

Figure 16: Suction Temperature Profiles: $\varepsilon^* = 0.05$, $\frac{\overline{x}}{L} = 1.0$

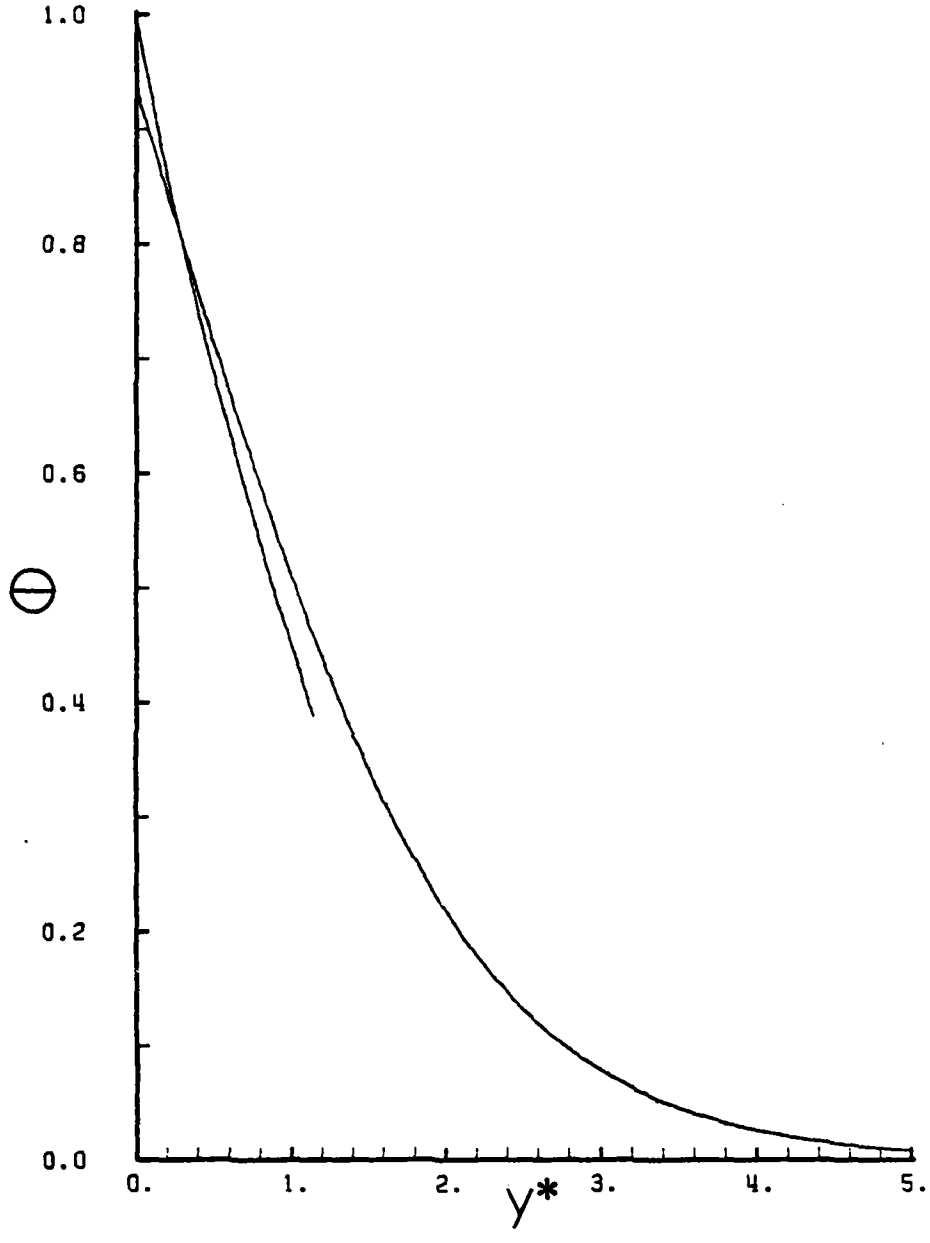

Figure 17: Suction Temperature Profiles: $\varepsilon^* = 0.25$, $\frac{\overline{x}}{L} = 0.25$

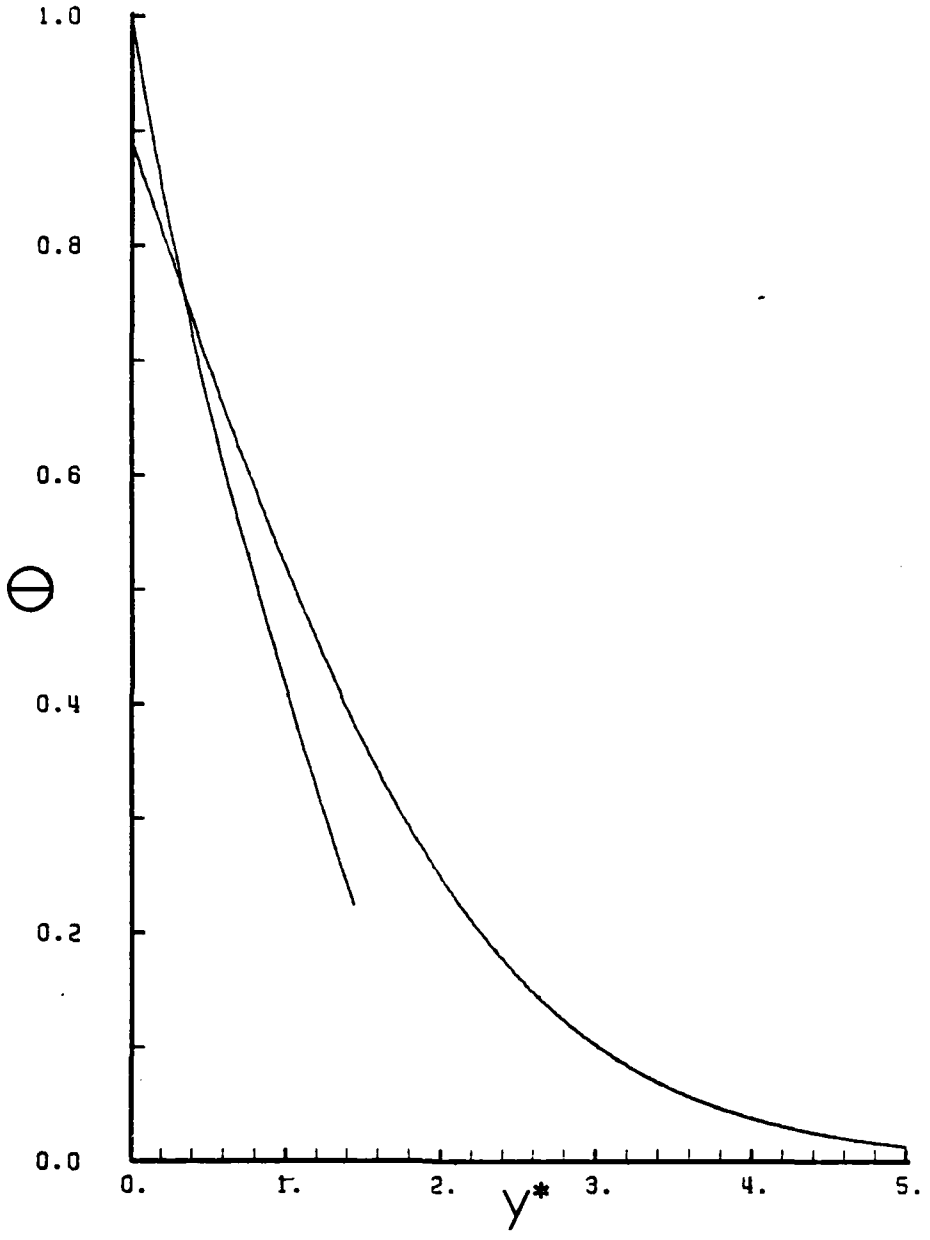

Figure 18: Suction Temperature Profiles: $\varepsilon^* = 0.25$, $\frac{\overline{x}}{L} = 0.50$

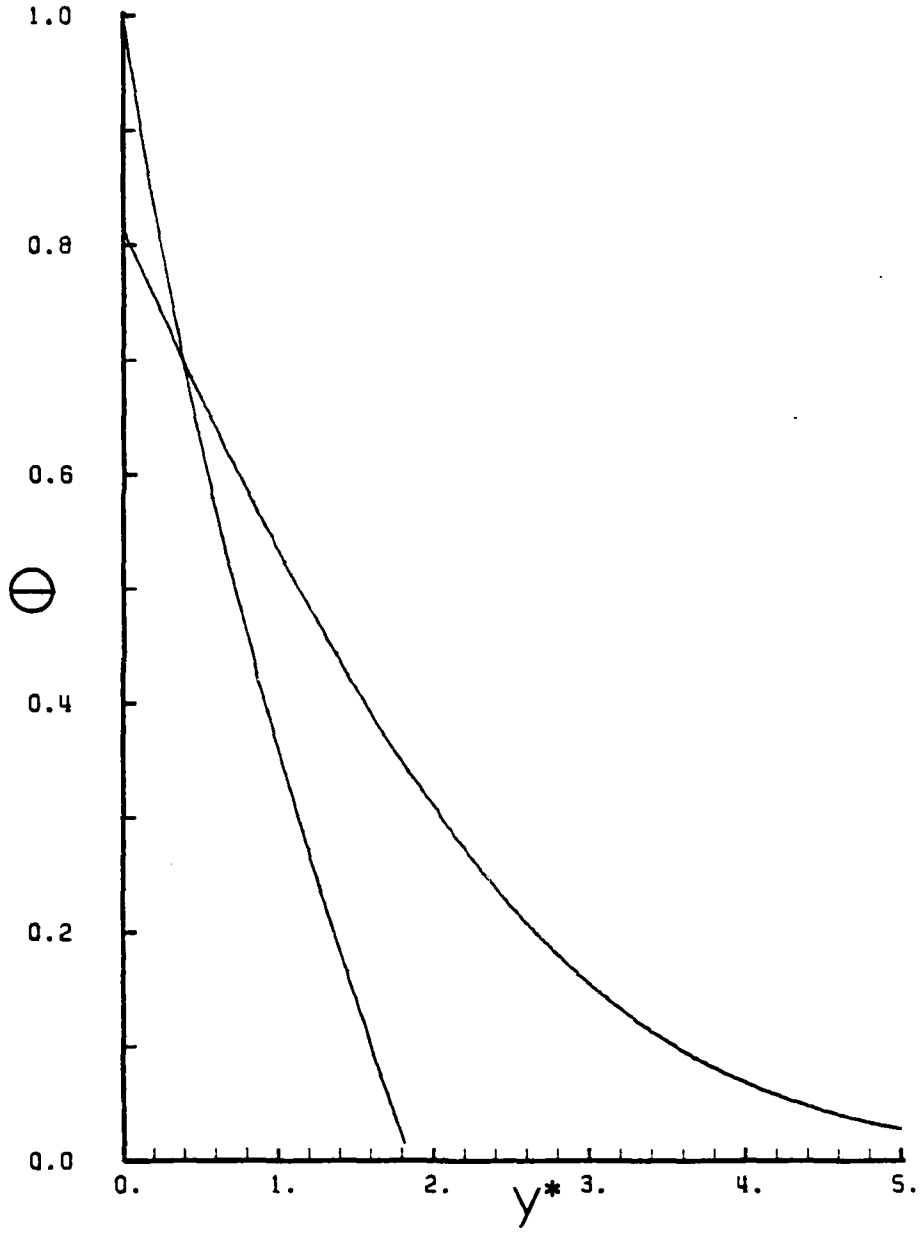

Figure 19: Suction Temperature Profiles: $\varepsilon^* = 0.25$, $\frac{\overline{x}}{L} = 1.0$

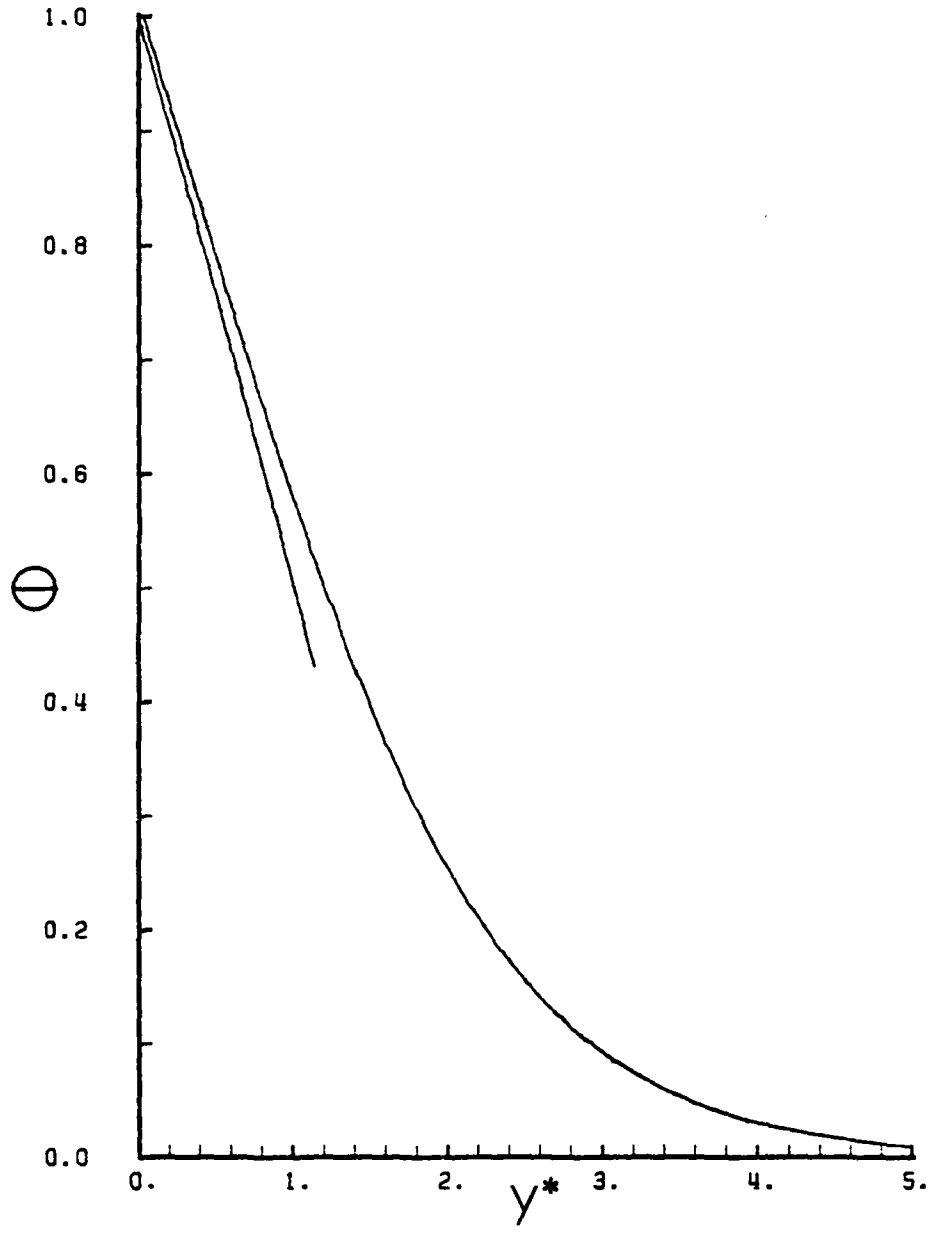

Figure 20: Blowing Temperature Profiles: $\varepsilon^* = -0.05$, $\frac{\bar{x}}{L} = 0.25$

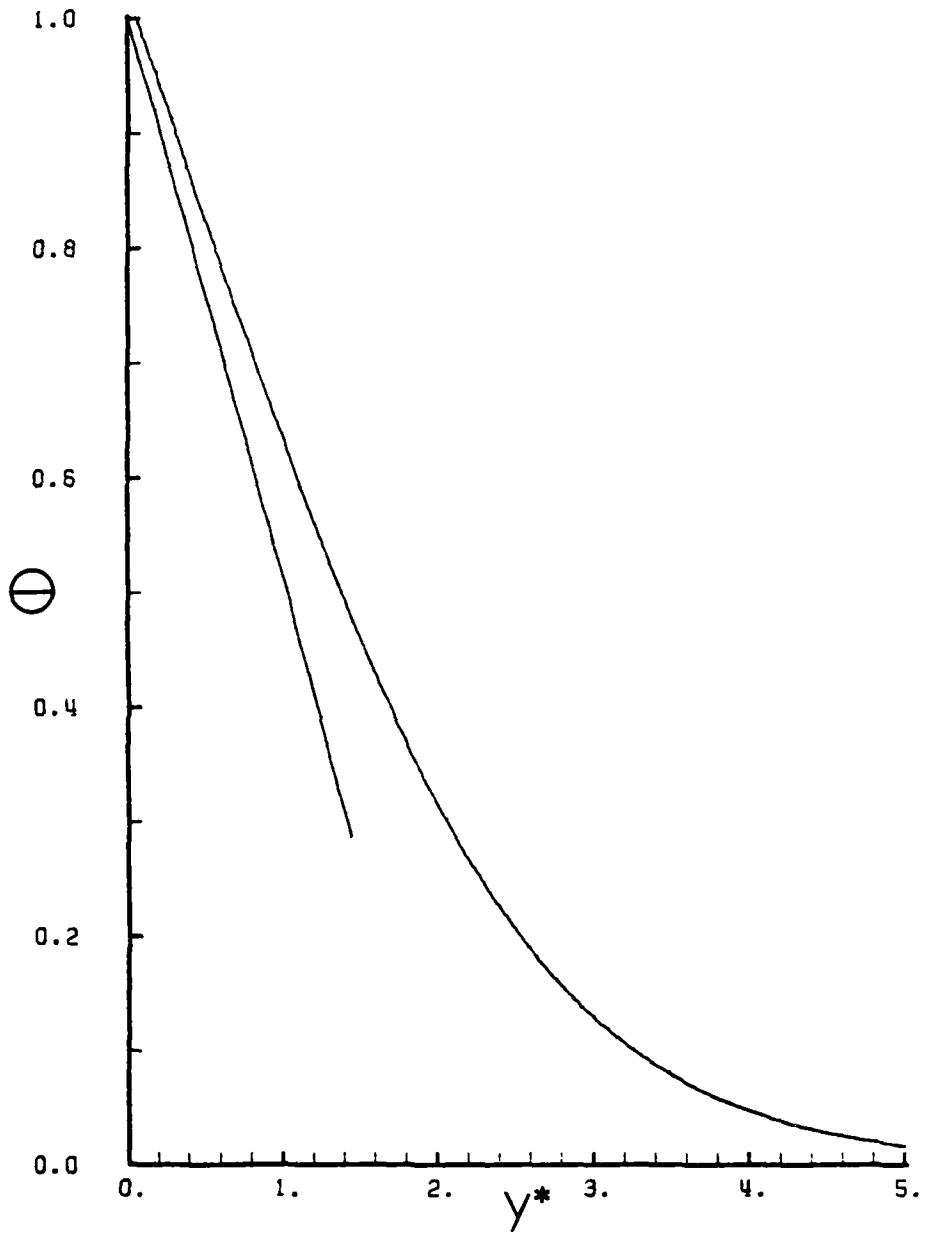

Figure 21: Blowing Temperature Profiles: $\varepsilon^* = -0.05$, $\frac{\bar{x}}{L} = 0.50$

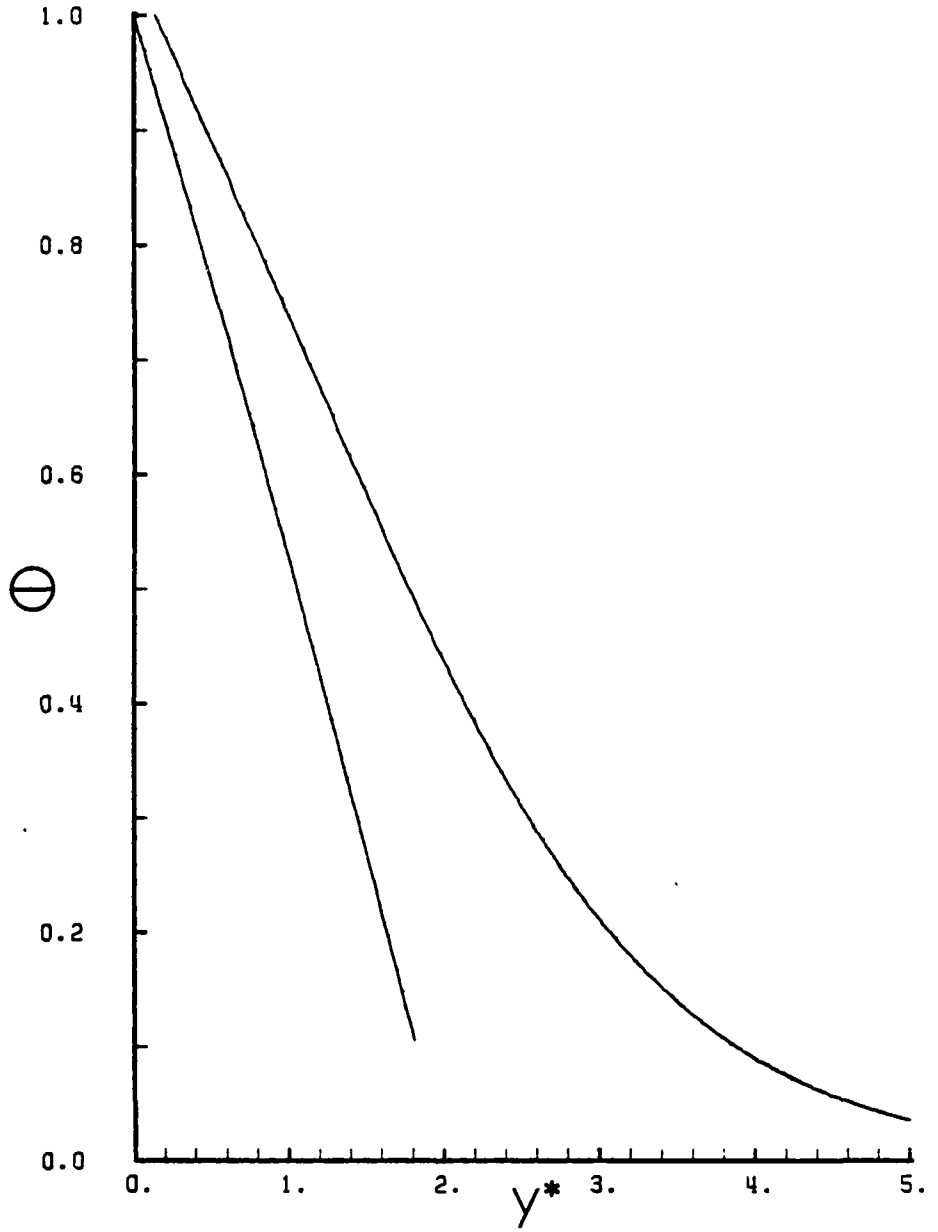

Figure 22: Blowing Temperature Profiles: $\varepsilon^* = -0.05$, $\frac{\bar{x}}{L} = 1.0$

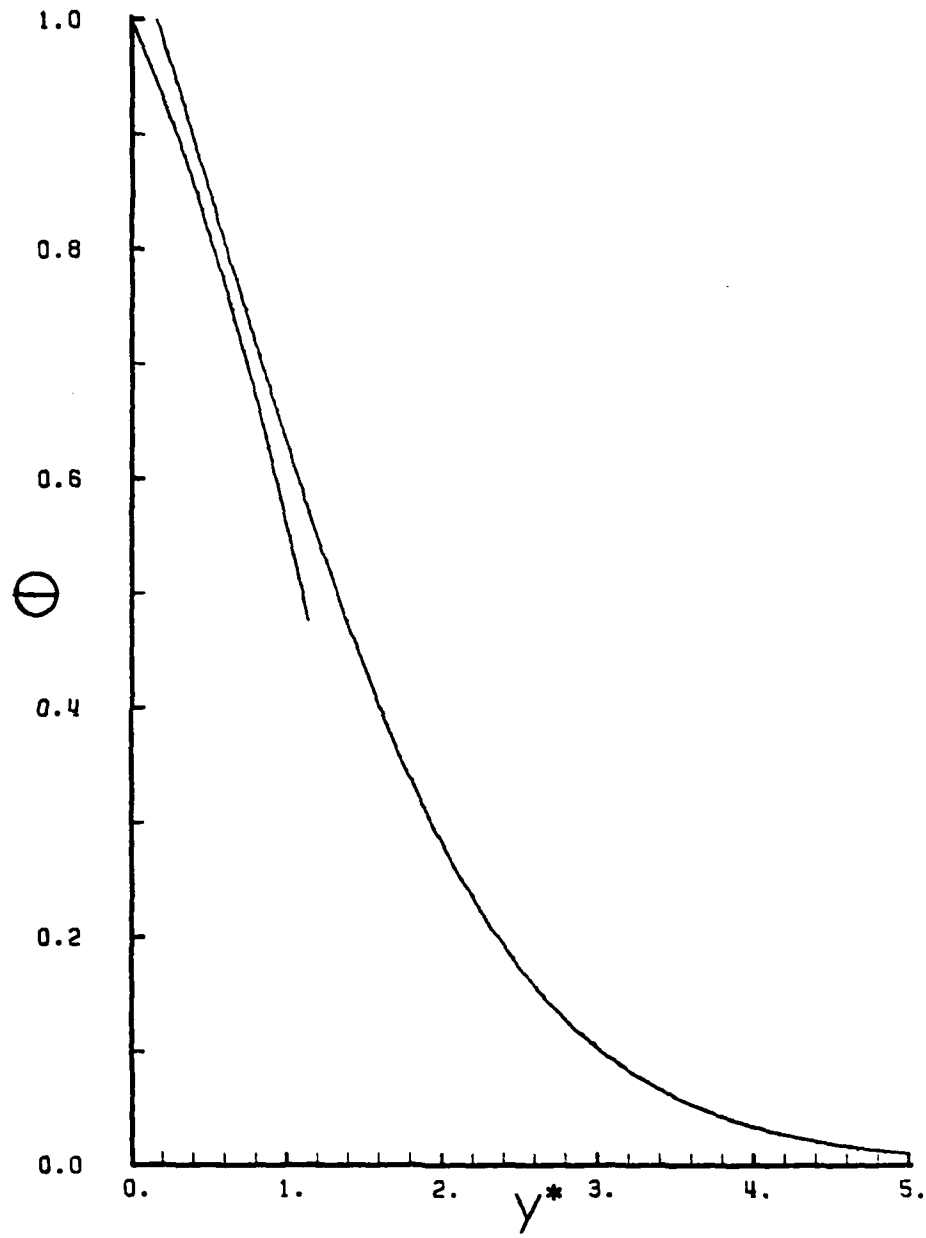

Figure 23: Blowing Temperature Profiles: $\varepsilon^* = -0.25$, $\frac{\bar{x}}{L} = 0.25$

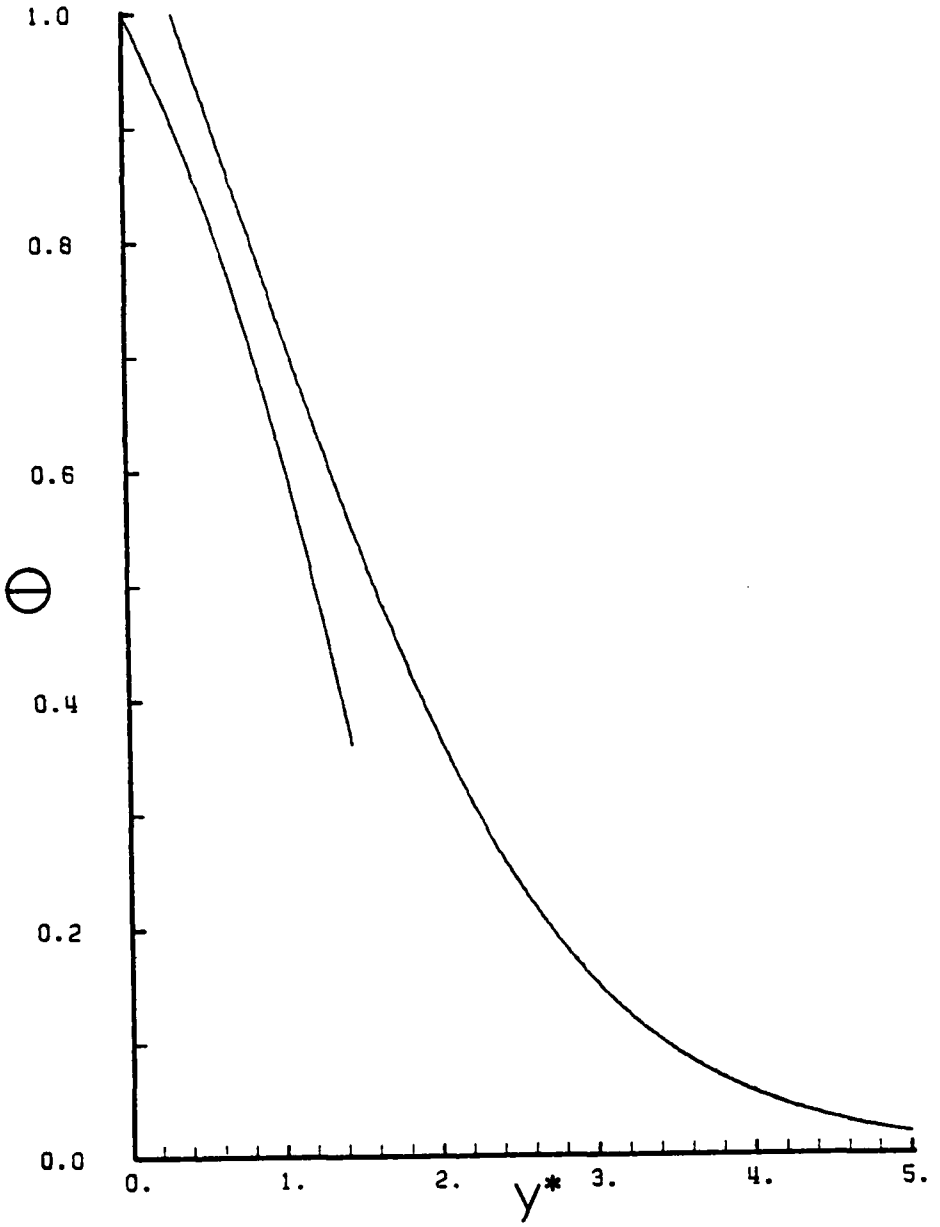

Figure 24: Blowing Temperature Profiles: $\varepsilon^* = -0.25$, $\frac{\bar{x}}{L} = 0.50$

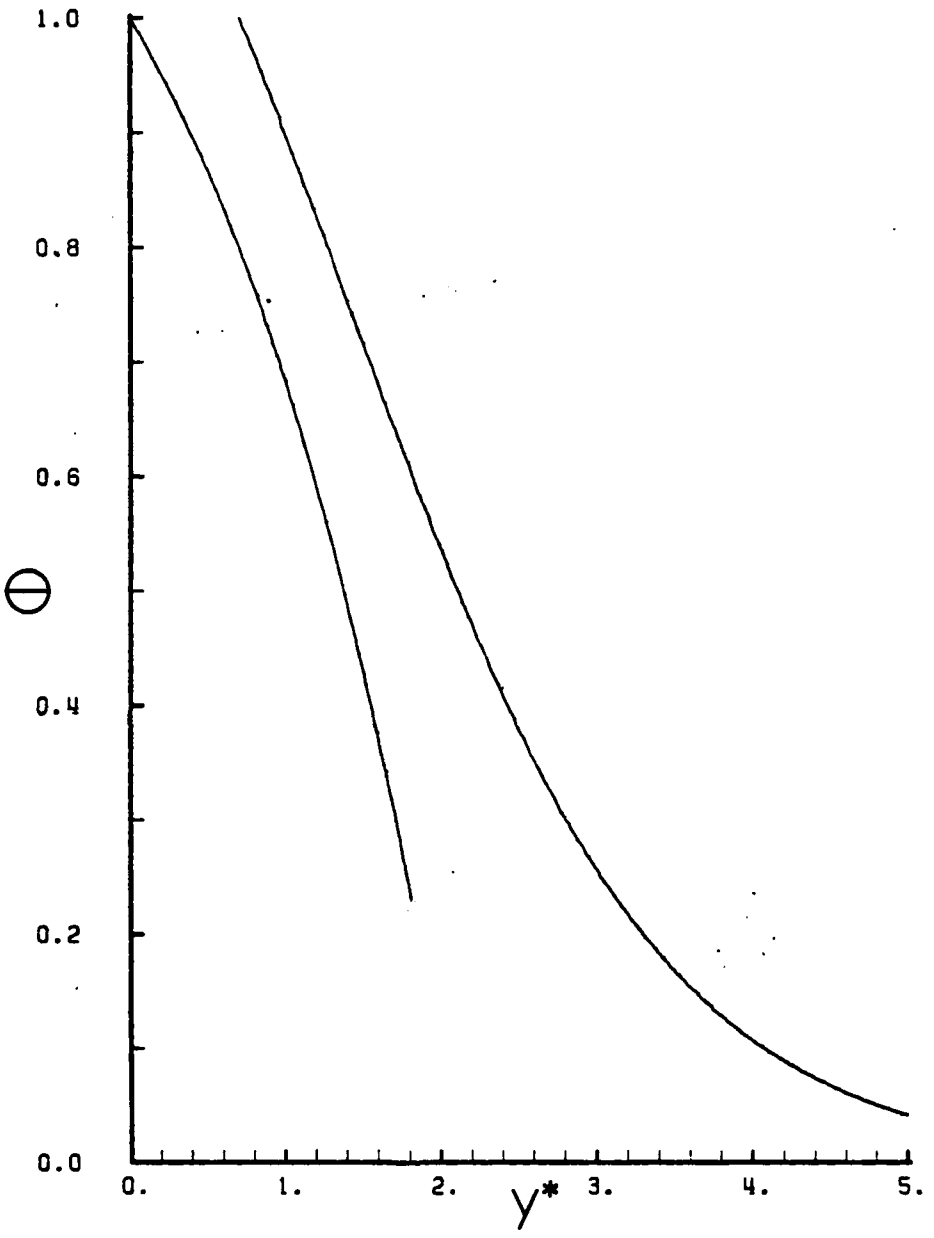

Figure 25: Blowing Temperature Profiles: $\varepsilon^* = -0.25$, $\frac{\overline{x}}{L} = 1.0$

3) Relative to the unperturbed free convection profiles the effect of suction for a given value of $\frac{\bar{x}}{L}$ is to increase the gradient.

4) For blowing the reverse effects of those outlined in 1) through 3) above are observed with the additional feature that the inner profiles are bowed out as well decreasing their gradient. This behavior characterizes a decreased heat transfer rate.

These observed phenomenon correspond with what physical intuition suggests should occur. In the case of suction heated fluid is moved closer to the wall thereby reducing the thickness of the thermal boundary-layer and enhancing the rate of heat transfer as is evidenced by the increase in gradient. The opposite situation in which blowing forces heated fluid farther from the plate causes the thermal boundary-layer to thicken. This creates an insulating effect which serves to reduce the rate of heat transfer evidenced by a decrease in gradient.

The outer temperature profiles again reflect the distinctive shape of unperturbed free convection profiles. In the case of suction their behavior is inconsistent and they do not behave relative to the free convection profiles as do the inner profiles. This again suggests that the effects of suction are most evident near the surface of the plate where the inner series is a closer approximation of the actual

behavior. For the case of blowing the outer profiles consistently move away from the plate with increases in either magnitude or distance above the discontinuity. Also, relative to the free convection profiles, they behave as expected moving farther out from the surface as the magnitude of blowing is increased for a specified value of $\frac{\bar{x}}{L}$. This suggests that the outer profiles are indeed a good approximation of temperature behavior at large distances from the plate.

4. Heat Transfer at the Surface of the Plate

In order to analyze the effects of discontinuous suction and blowing on the rate of heat transfer at the plate a graphical comparison was made of the following three physical situations:

1) Unperturbed free convection from an isothermal plate.
2) Free convection from an isothermal plate with continuous suction or blowing applied over the entire length. (from the study by Sparrow and Cess [7].
3) Free convection from an isothermal plate with discontinuous suction or blowing applied at a distance L above the leading edge.

For each of these cases the heat transfer data was correlated according to following nondimensional parameter:

$$Nu\ (Gr/4)^{-\frac{1}{4}} \qquad (46)$$

where the Nusselt number in each case Nu_0, Nu, and Nu_1 was evaluated according to length scale associated with the discontinuity; i.e., L. The three parameters have the following form:

$$1)\quad Nu_0(Gr/4)^{-\frac{1}{4}} = -H'(0)(x+1)^{-\frac{1}{4}} \tag{47}$$

$$2)\quad Nu_1(Gr/4)^{-\frac{1}{4}} = -H'(0)(x+1)^{-\frac{1}{4}} - 1.40\varepsilon^* \tag{48}$$

$$3)\quad Nu(Gr/4)^{-\frac{1}{4}} = -[H'(0) + (Z'_{10}(0) + \varepsilon^* Z'_{11}(0)\xi + (Z'_{20}(0) + \varepsilon^* Z'_{21}(0) + \varepsilon^{*2} Z'_{22}(0))\xi^2] \tag{49}$$

The heat transfer parameters were plotted as functions of x, i.e., $\frac{\bar{x}}{L}$, for suction and blowing magnitudes, ε^*, of .05 and .25 in Figures (26)-(29). As expected in the region from the leading edge, $\bar{x} = -L$, to the discontinuity at $x = 0$ the heat transfer rates for cases 1) and 3) are identical and in case 2) the rate is higher by a fixed amount over the unperturbed free convection case. At the discontinuity the curve for the discontinuous case experiences an abrupt change in slope and intersects the continuous case curve at approximately $\frac{\bar{x}}{L} = 0.22$ for $\varepsilon^* = 0.05$ and at $\frac{\bar{x}}{L} = 0.52$ for $\varepsilon^* = 0.25$. The magnitude of applied suction apparently has a significant effect on the location of the crossover point where the discontinuous heat transfer rate exceeds that for the continuous case. The behavior of the discontinuous heat transfer rate as $\frac{\bar{x}}{L}$ increases does not appear to approach an asymptotic suction limit characteristic of a constant boundary-layer thickness. However, since the inner temperature series expansion constructed to approximate behavior near the surface is only valid in the

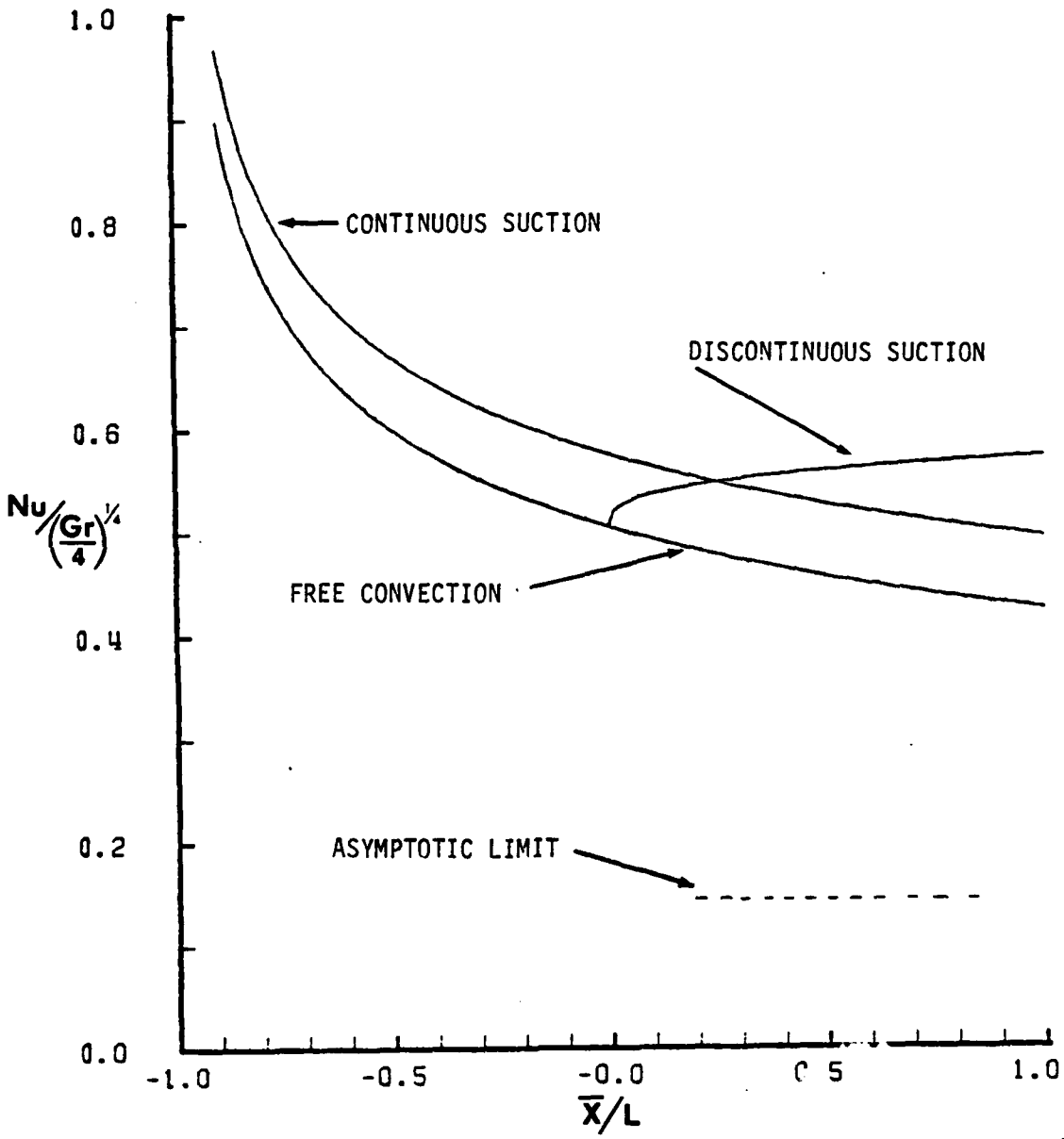

Figure 26: Comparison of Heat Transfer at the Surface of the Plate with Suction, $\varepsilon^* = 0.05$.

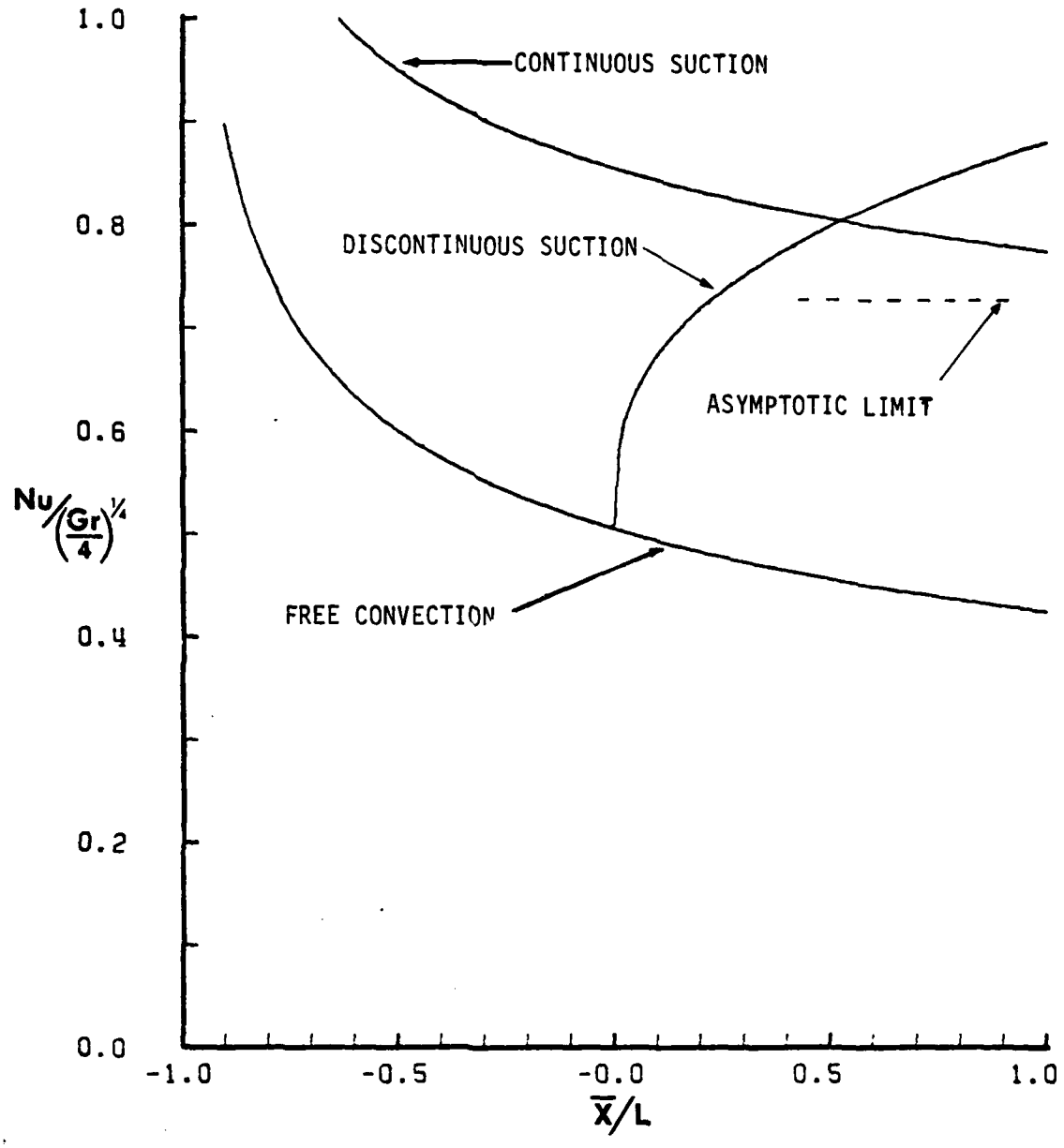

Figure 27: Comparison of Heat Transfer at the Surface of the Plate with Suction, $\varepsilon^* = 0.25$.

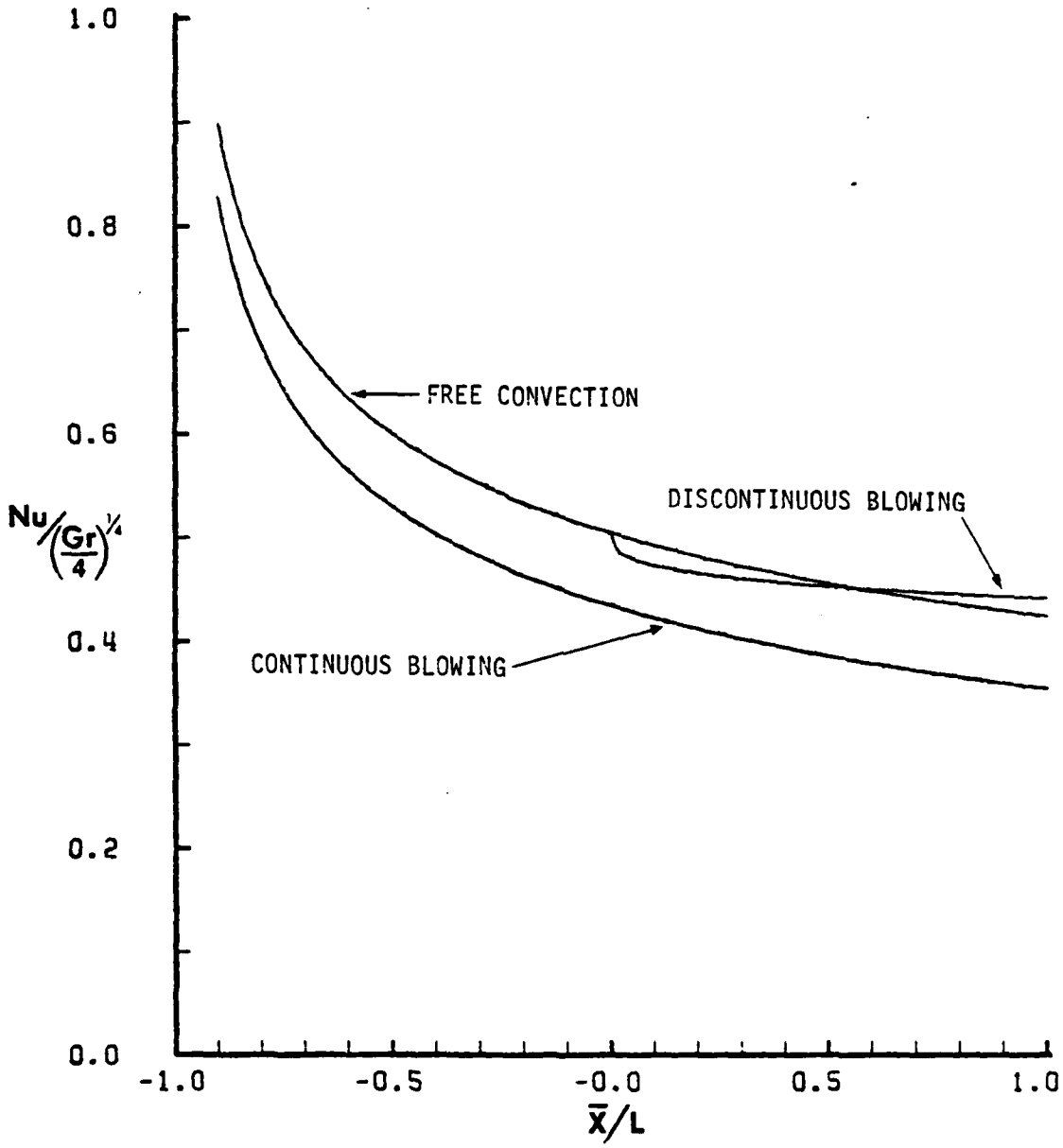

Figure 28: Comparison of Heat Transfer at the Surface of the Plate with Blowing, $\varepsilon^* = -0.05$.

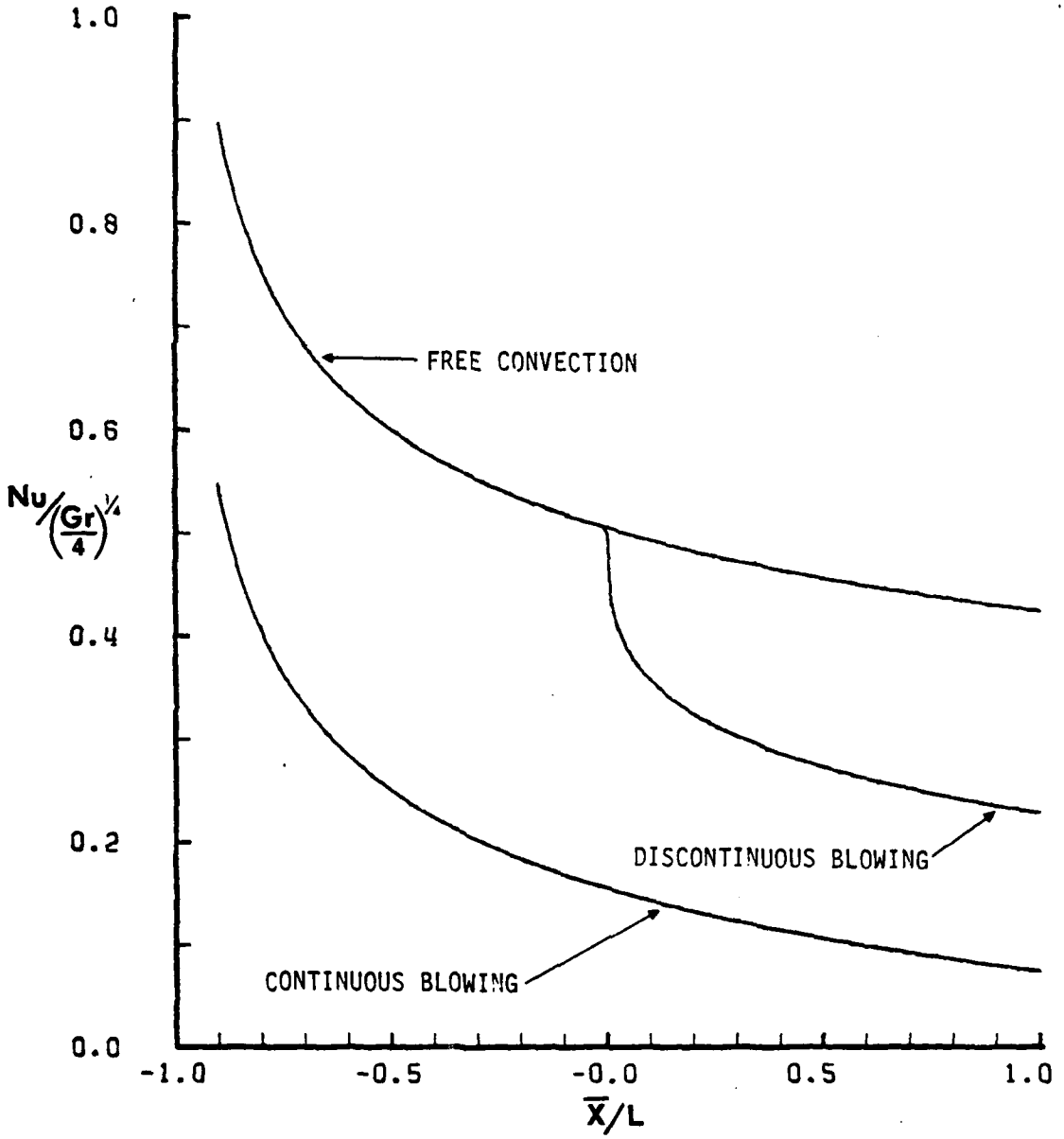

Figure 29: Comparison of Heat Transfer at the Surface of the Plate with Blowing, $\epsilon^* = -0.25$.

neighborhood of the discontinuity, i.e., small values of $\frac{\bar{x}}{L}$, it cannot be expected to accurately predict results in asymptotic limiting case as $\frac{\bar{x}}{L}$ becomes large. The addition of higher terms to the inner expansion would serve to extend the range of validity, however, since the Sparrow and Cess analysis of the continuous case employed only first order terms, it is reasonable to expect the results of the present analysis to provide a closer approximation to the physical situation. This essential difference between the two studies should be kept in mind when comparing results. The situation with blowing applied as depicted in Figures (28) and (29) shows the expected reduction in heat transfer rates when compared to the unperturbed free convection in both the continuous and discontinuous cases. At the discontinuity, however, the curve representing discontinuous blowing exhibits a downward shift in slope and then follows a path which is basically parallel to the free convection and continuous blowing curves. The crossover that occurs in the case of a blowing magnitude of $\varepsilon^* = -0.05$, is probably an anomaly due to an insufficient number of terms in both the continuous and discontinuous series expansions. For a blowing parameter of $\varepsilon^* = -0.25$ all three curves appear to asymptotically approach the same slope. A final judgement as to the degree of accuracy with which the present analysis models the heat transfer behavior with discontinuous blowing or suction applied must await comparison with experimental data.

V. CONCLUSIONS AND RECOMMENDATIONS

An overall review of the results obtained from this analysis leads to a number of general conclusions. An apparent range of validity for the expansions can be estimated from a comparison of the inner and outer profiles presented in Figures 2-25 based on the degree of correlation between them. In terms of the streamwise distance from the discontinuity a qualitative upper bound of $\frac{\bar{x}}{L} = 1.0$ is suggested. In terms of the blowing and suction parameter the relationship given on equation (44) suggests an upper limit of $|\varepsilon^*| = 1.0$ which equates to a magnitude of approximately .05 $\bar{u}_{max}$ for $\bar{v}_w$ for which the original boundary layer equations should remain valid. In the case of suction the inner profiles appeared to model the expected behavior of the location and magnitude of the maximum velocity with respect to the unperturbed free convection profiles better than did the outer profiles. When blowing was applied, the outer profiles correlated with anticipated behavior in this respcet better than the inner profiles. In general the matching of the inner and outer velocity profiles improves as the streamwise distance from the discontinuity decreases and is also qualitatively better in the blowing cases. The analysis also indicated that while the inner series provides reasonably good results at very small distances from the plate, in an overall integrated sense the outer profiles exhibit a closer correlation

with the velocity behavior associated with free convection.

The effects of suction and blowing on the temperature distribution both appear to be well modeled by the inner series expansions. Again the degree of matching between the inner and outer profiles significantly improves as the streamwise distance from the discontinuity decreases. Also the effects of the discontinuity on temperature behavior, relative to the free convection case, are less direct than on velocity behavior. This difference is evidenced in the manner of coupling exhibited by the ordinary differential equations which define the inner expansion coefficient functions (see equations (19) and (20)). This fact in addition to the apparent overestimate of velocity magnitudes produced by the outer series; the underestimate by the inner series; and the heat transfer behavior predicted for small suction magnitudes suggest that additional higher order terms be added to both inner and outer expansions to achieve a better approximation of the physical situation. In general the results obtained for the effects of discontinuous suction or blowing on heat transfer at the surface of the plate seemed consistent with the results for unperturbed free convection and the case of continuous suction or blowing applied over the entire plate length. Comparison with experimental data when it becomes available will enable a more definitive conclusion to be made regarding the validity of this solution with respect to heat transfer performance.

Also, with the addition of higher order terms to the inner series it would be possible to determine if the heat transfer results predicted by the present analysis tend to approach the asymptotic limits for large values of $\frac{\bar{x}}{L}$ established by Merkin [9]. In that study the following asymptotic limits for continuous suction and blowing at large distance from the leading edge were reported, given below in terms of the parameters used in this analysis:

1) For suction $Nu/(\frac{Gr}{4})^{\frac{1}{4}} \rightarrow 4\varepsilon * Pr$ as $\frac{\bar{x}}{L} \rightarrow \infty$

2) For blowing $Nu/(\frac{Gr}{4})^{\frac{1}{4}} \rightarrow 0$ as $\frac{\bar{x}}{L} \rightarrow \infty$

The asymptotic limit in the case of suction is represented by the dashed line in Figures (26) and (27).

Although an exact determination of the inner-outer series match point is not essential when the primary interest of the investigation is to predict behavior at the surface of the plate, a more rigorous determination of that point would serve to enhance the overall creditability of the present method of solution. Therefore, another recommendation to improve the method point is to use the energy balance integral given in (42) to form an energy difference, i.e., from a difference integral by substracting the right side from the left side. A numerical minimization procedure could then be applied to this difference to determine the match point which most closely satisfies the energy balance.

APPENDIX A

CONSTRUCTION OF THE FREE CONVECTION MATCHING SERIES

The equations which define the behavior of the free convection velocity and temperature profiles were presented in equations (9a) and (9b), with appropriate boundary conditions, in terms of similarity functions F and H which characterize the stream function and temperature distribution respectively. In the region near the surface of the plate, $y^* = 0$, and at the location of the discontinuity, $x = 0$, these functions can be approximated by suitable series expansions in powers of y^* as follows:

$$F(y^*) = \sum_{j=o} a_j (y^*)^j \tag{A-1}$$

$$H(y^*) = 1 + \sum_{j=1} b_j (y^*)^j \tag{A-2}$$

where the variable y^* can be used since it is identically equal to the free convection similarity variable at $x = 0$.

The constant coefficients in (A-1) and (A-2) can be determined from applying the following previously enumerated boundary conditions:

$$\begin{aligned} &\text{At } y^* = 0: && F(0) = 0 \\ & && F'(0) = 0 \\ & && H(0) = 1 \\ &\text{As } y^* \to \infty: && F'(\infty) = 0 \\ & && H(\infty) = 0 \end{aligned} \tag{A-3}$$

These conditions immediately yield the result that $a_0 = a_1 = 0$. By evaluating the series representations for F'' and H' the constants a_2 and b_1 are specified as:

$$a_2 = \tfrac{1}{2}F''(0) \text{ and } b_1 = H'(0)$$

where both of these initial values are well known and depend only the Prandtl number.

To evaluate the higher order coefficients the form for F''' must be obtained from equation (9a):

$$F''' = -3FF'' + 2F'^2 - H$$

which when evaluated at $y^* = 0$ yields $F'''(0) = -1$ and equating this value to the series form of F''' yields:

$$a_3 = -\frac{1}{6}$$

A similar technique is used in determining b_2 from equation (9b) and the following value is obtained:

$$b_2 = 0$$

The remainder of the coefficients are found by successively differentiating equations (9a) and (9b) and equating them to the appropriate series representation evaluated at $y^* = 0$. The results of this process are summarized below:

$$\begin{aligned} a_0 &= 0 & b_1 &= H'(0) \\ a_1 &= 0 & b_2 &= 0 \\ a_2 &= \tfrac{1}{2}F''(0) & b_3 &= 0 \\ a_3 &= -1/6 & b_4 &= \frac{-PrF''(0)\,H'(0)}{8} \end{aligned} \qquad \text{(A-4)}$$

$$a_4 = \frac{-H'(0)}{24}$$

$$a_5 = \frac{[F''(0)]^2}{120}$$

These series forms for F and H will be used to satisfy the matching conditions for both the inner and outer expansions later in the course of the analysis.

APPENDIX B

DETERMINATION OF THE STREAM FUNCTION AND TEMPERATURE DISTRIBUTION SERIES EXPANSION PARAMETERS

Recalling that the definitions of the stream function and temperature profile series expansions involved certain arbitrary constants, the methods and procedures used in evaluating them are outlined in this appendix.

$$\psi = \varepsilon^*(\xi/\phi_1)^{\frac{1}{a}} + \phi_3\xi^c[\xi^k f_f(\eta)] \tag{B-1}$$

$$\theta = 1 + \phi_4\xi^d[\xi^k g_k(\eta)] \tag{B-2}$$

where

$$\xi = \phi_1 x^a \text{ and } \eta = \phi_2 y^* x^b \tag{B-3}$$

The object of constructing such expansions for the stream function and temperature distribution is to obtain series representations which satisfy the momentum and energy equations which mathematically model the physical problem. The individual components of those governing equations (6) and (7), i.e., the partial derivatives, must be evaluated in terms of expressions (B-1) through (B-3). Substituting (B-1) and (B-2) into the momentum and energy equations yields:

Momentum Equation

$$4\phi_1^{\frac{1-2b}{a}}\phi_2^2\phi_3\xi^{2c} + \frac{2b-1}{a}\{[a(c+k)+b)\xi^k f_k'][\xi^k f_k']$$

$$- [a(c + k)\xi^k f_k][\xi^k f_k''] \} - 4\varepsilon^* \phi_1^{-\frac{2b}{a}} \phi_2^2 \phi_3 \xi^{c + \frac{2b}{a}} [\xi^k f_k'']$$

$$= \phi_1^{-\frac{3b}{a}} \phi_2^3 \phi_3 \xi^{c + \frac{3b}{a}} [\xi^k f_k'''] + 1 + \phi_4 [\xi^k g_k] \qquad \text{(B-4)}$$

Energy Equation

$$4\phi_1^{\frac{1-b}{a}} \phi_2 \phi_3 \phi_4 \xi^{c+d+\frac{b-1}{a}} \{[a(d + k)\xi^k g_k][\xi^k f_k']$$

$$- [a(c + k)\xi^k f_k][\xi^k g_k'] \} - 4\varepsilon^* \phi_1^{-\frac{b}{a}} \phi_2 \phi_4 \xi^{\frac{b}{a} + d} [\xi^k g_k']$$

$$= \frac{1}{Pr_1} \phi_1^{-\frac{2b}{a}} \phi_2^2 \phi_4 \xi^{\frac{2b}{a} + d} [\xi^k g_k''] \qquad \text{(B-5)}$$

Certain conditions which must be satisfied will impose restrictions on the allowable values for the ϕ's and constants a, b, c and d. The one condition which must be satisfied by the equations is the initial velocity and temperature matching at a distance L from the leading edge of the plate where the discontinuity in normal velocity begins. At this location the perturbed velocity and temperature profiles must match the free convection profiles. In terms of the stream function the velocity is given by:

$$u^* = \frac{\partial \psi}{\partial y^*} = \phi_1^c \phi_2^{-\frac{ca}{b}} \phi_3 \left(\frac{y^*}{\eta}\right)^{-\frac{ac}{b} - 1} [\phi_1^k \phi_2^{-\frac{ka}{a}} \left(\frac{y^*}{\eta}\right)^{-\frac{ka}{b}} f_k'] \qquad \text{(B-6)}$$

The free convection velocity profile written in terms of u* can be expressed as follows:

$$u^* = F'[y^*] = \sum_{j=2} j a_j (y^*)^{j-1} \qquad \text{(B-7)}$$

Equating the leading term in each series (B-6) and (B-7) i.e., when j=2 and k=0 we obtain the following relationship:

$$2a_2 y^* = \phi_1^c \phi_2^{-\frac{ca}{b}} \phi_3 \left(\frac{y^*}{\eta}\right)^{-\frac{ac}{b}-1} f_0' \qquad \text{(B-8)}$$

For proper matching, the exponents of y* must be equal; therefore,

$$-\frac{ac}{b} - 1 = 1 \qquad \text{(B-9)}$$

Also, since it is desirable to have expressions which are independent of ε^* for the boundary conditions on the f_k as $\eta \to \infty$, the following condition will be imposed:

$$\phi_1^c \phi_2^{-\frac{ca}{b}} \phi_3 = 1 \qquad \text{(B-10)}$$

The requirements for matching the temperature profiles yields:

$$\phi_1^c \phi_2^{-\frac{ad}{b}} \phi_4 \left(\frac{y^*}{\eta}\right) \left[\phi_1^k \phi_2^{-\frac{ka}{b}} \left(\frac{y^*}{\eta}\right)^{-\frac{ka}{b}} g_k\right] = \sum_{j=1} b_j y^{*j} \qquad \text{(B-11)}$$

Applying similar arguments to those used for the condition of velocity matching, the following relationships are obtained from (B-11):

$$-\frac{ad}{b} = 1 \qquad \text{(B-12)}$$

and

$$\phi_1^d \phi_2 \phi_4 = 1 \qquad \text{(B-13)}$$

For additional restrictions on the exponent constants consider equation (B-4) in which the highest order derivative term must appear in the 0th order expansion in order to obtaine meaningful results. This requirement imposes the following condition on the exponents of ξ:

$$c + \frac{3b}{a} \leq 2c + \frac{2b-1}{a}$$

or equivalently,

$$ac \geq b + 1 \tag{B-14}$$

The same restriction also applies to the energy expansion, equation (B-5) and the same relationship is obtained (B-14). Since fractional exponents on ξ are not permissable, due to the inability to match coefficients of like of powers of ξ in both expansions, from equation (B-12) the following further information is obtained:

$$d = 1 \tag{B-15}$$

and

$$-\frac{a}{b} = 1 \tag{B-16}$$

Now combining (B-9) and (B-16), the constant c is specified as:

$$c = 2 \tag{B-17}$$

Using this information and the relationship given in (B-14) imposes the following restrictions on the possible values of a and b:

$$a \geq 1/3 \text{ and } b \leq -1/3 \tag{B-18}$$

The relationships previously obtained for the ϕ's can be simplified by substituting the known values for the exponents in equations (B-10) and (B-13) from which are obtained the following:

$$\phi_1^2 \phi_2^2 \phi_3 = 1 \tag{B-19}$$

and

$$\phi_1 \phi_2 \phi_4 = 1 \tag{B-20}$$

Since equation (B-5) is homogeneous in ϕ_4 and ϕ_4 appears only singly in equation (B-4), without loss of generality it can be set equal to unity. Setting $\phi_4 = 1$ in equations (B-19) and (b-20) yields the following further relationships for the ϕ's:

$$\phi_1 \phi_2 = 1 \tag{B-21}$$

and

$$\phi_3 = 1 \tag{B-22}$$

The foregoing analysis has permitted the reformulation of equations (B-4) and (B-5) in terms of only two unspecified parameters a and ϕ_1, and those equations reduce to the following forms:

$$\text{Momentum: } 4a\phi_1 \xi^{\frac{1}{a}3-\frac{1}{a}}\{[k+1)\xi^k f_k'][\xi^k f_k'] - [(k+2)\xi^k f_k]\cdot [\xi^k f_k'']\} - 4\epsilon^*\xi[\xi^k f_k''] = [\xi^k f_k'''] + \xi + \xi^2[\xi^k g_k] \tag{B-23}$$

$$\text{Energy: } 4a\phi_1 \xi^{\frac{1}{a}3-\frac{1}{a}}\{[(k+1)\xi^k g_k][\xi^k f_k'] - [(k+2)\xi^k f_k]\cdot [\xi^k g_k']\} - 4\epsilon^*\xi[\xi^k g_k'] = \frac{1}{Pr}[\xi^k g_k''] \tag{B-24}$$

Equation (B-18) allows for only two reasonable choices for the value of a; namely, a = 1/3 or a = 1/2. Furthermore, for each of these two values ϕ_1 can be defined to either include ϵ^* or not; thereby posing four possible cases for consideration. The cases which specify a = 1/2 do not satisfy the boundary condition for f_1 as $\eta \to \infty$; and therefore, are unacceptable for the present problem. The case for which ϵ^* is included in ϕ_1 and a = 1/3 results in a set of ordinary differential equations

which include ε^* in the homogeneous part and which cannot be transformed into general equations independent of ε^* through the use of universal functions. Therefore, the case with $a = 1/3$ and ε^* not included in the definition of ϕ_1 was selected to complete the solution of the problem. A summary of the results is presented below:

$$a = 1/3,\ b = -1/3,\ c=2,\ d = 1 \tag{B-25}$$

$$\phi_1 = (\tfrac{3}{4})^{1/3},\ \phi_2 = (\tfrac{3}{4})^{-1/3},\ \phi_3 = \phi_4 = 1 \tag{B-26}$$

$$\xi = (\tfrac{3}{4}x)^{1/3},\ \eta = (\tfrac{3}{4}x)^{-1/3} y^* = y^*/\xi \tag{B-27}$$

$$\psi = \frac{4}{3}\varepsilon^*\xi^3 + \xi^2[\xi^k f_k] \tag{B-28}$$

$$\theta = 1 + \xi[\xi^k g_k] \tag{B-29}$$

The momentum and energy expansions which result from these definitions were presented in Chapter II, equations (17) and (18). All that remains is to specify the appropriate boundary conditions for the f_k and g_k.

At $\eta = 0$: $u^* = \frac{\partial\psi}{\partial y^*} = \xi[\xi^k f_k'] = 0,$ (B-30)

$$v^* = -\frac{\partial\psi}{\partial x} = -[\varepsilon^* + \frac{1}{4}\xi^{-1}[(k+2)\xi^k f_k]\} = \pm\varepsilon^*, \tag{B-31}$$

and

$$\theta = 1 + \xi[\xi^k g_k] = 1 \tag{B-32}$$

From these original boundary conditions, the local boundary conditions for f_k and f_k' are determined to be:

$$f_k(0) = f_k'(0) = g_k(0) = 0, \text{ for all } k \tag{B-33}$$

The boundary conditions at $\eta\to\infty$ are obtained through matching the velocity and temperature profiles to the free convection

profiles. The velocity match is performed by equating equations (B-6) and (B-7) with the appropriate values substituted for the unspecified parameters. The result of this process is the following relationship:

$$\sum_{j=2} j a_j (y^*)^{j-1} = [(\frac{y^*}{\eta})^{k+1} f'_k] \qquad \text{(B-34)}$$

By equating like powers of y^* and substituting the values for the a_j obtained in Appendix A the following local boundary conditions for the f'_k as $\eta \to \infty$ are determined:

$$\begin{aligned}
\frac{f'_0}{\eta^1} &= 2a_2 = F''(0) \quad \text{as } \eta \to \infty \\
\frac{f'_1}{\eta^2} &= 3a_3 = -\frac{1}{2} \quad \text{as } \eta \to \infty \\
\frac{f'_2}{\eta^3} &= 4a_4 = -\frac{H'(0)}{6} \quad \text{as } \eta \to \infty \\
\frac{f'_3}{\eta^4} &= 5a_5 = \frac{[F''(0)]^2}{24} \quad \text{as } \eta \to \infty
\end{aligned} \qquad \text{(B-35)}$$

The temperature profile matching yields the following local boundary conditions for the g_k:

$$\begin{aligned}
\frac{g_0}{\eta} &= b_1 = H'(0) \quad \text{as } \eta \to \infty \\
\frac{g_1}{\eta^2} &= b_2 = 0 \quad \text{as } \eta \to \infty \\
\frac{g_2}{\eta^3} &= b_3 = 0 \quad \text{as } \eta \to \infty \\
\frac{g_3}{\eta^4} &= b_4 = -\frac{PrF''(0)H'(0)}{8} \quad \text{as } \eta \to \infty
\end{aligned} \qquad \text{(B-36)}$$

APPENDIX C

THIRD ORDER UNIVERSAL FUNCTION EQUATIONS

The third order ordinary differential equations which result from the expansions given in (17) and (18) are presented below, although only functions of second order and lower were employed in the actual analysis:

$$f_3''' + 2f_0 f_3'' - 5f_0' f_3' + 5f_0'' f_3 = 5f_1' f_2' - 3f_1' f_2'' - 4f_1'' f_2 - 4\varepsilon^* f_2'' - g_1 \qquad \text{(C-1)}$$

$$\frac{1}{Pr} g_3'' + 2f_0 g_3' - 4f_0' g_3 + 5g_0' f_3 - g_0 f_3' = 2g_1 f_3' + 3g_2 f_1' - 3f_1 g_2' - 4f_2 g_1' - 4\varepsilon^* g' \qquad \text{(C-2)}$$

The corresponding forms for f_3 and g_3 in terms of the universal functions and the resulting differential equations are as follows:

$$f_3 = Y_{30} + \varepsilon^* Y_{31} + \varepsilon^{*2} Y_{32} + \varepsilon^{*3} Y_{33} \qquad \text{(C-3a)}$$

and

$$g_3 = Z_{30} + \varepsilon^* Z_{31} + \varepsilon^{*2} Z_{32} + \varepsilon^{*3} Z_{33} \qquad \text{(C-3b)}$$

The third order momentum equation becomes:

$$M_3[Y_{30}] = 5Y_{10}' Y_{20}' - 3Y_{10} Y_{20}'' - 4Y_{10}'' Y_{20} - Z_{10}; \qquad \text{(C-4a)}$$

$$M_3[Y_{31}] = 5Y_{11}' Y_{20}' + 5Y_{10}' Y_{21}' - 3Y_{10} Y_{21}'' - 3Y_{11} Y_{20}''$$

AD-A104 055 NAVAL POSTGRADUATE SCHOOL MONTEREY CA F/G 20/4
FREE CONVECTION FROM A SEMI-INFINITE VERTICAL PLATE WITH DISCON--ETC(U)
MAR 81 W A SCHIESSER

UNCLASSIFIED NL

2 of 2
AD A104 055

END
DATE FILMED
10-81
DTIC

$$- 4Y''_{10}Y_{21} - 4Y''_{11}Y''_{20} - Z_{11}; \qquad \text{(C-4b)}$$

$$M_3[Y_{32}] = 5Y'_{10}Y'_{22} + 5Y'_{11}Y'_{21} - 3Y_{10}Y''_{22} - 3Y_{11}Y''_{21}$$

$$- 4Y''_{10}Y_{22} - 4Y''_{11}Y_{21} - 4Y''_{21}; \qquad \text{(C-4c)}$$

$$M_3[Y_{33}] = 5Y'_{11}Y'_{22} - 3Y_{11}Y''_{22} - 4Y''_{11}Y_{22} - 4Y''_{22} \qquad \text{(C-4d)}$$

where the linear differential operator M_3 is defined by:

$$M_3 = Y'''_3 + 2f_0Y''_3 - 5f'_0y'_3 + 5f''_0y_3 \qquad \text{(C-4e)}$$

The third order energy equation becomes:

$$E_3[Z_{30}] = 2Z_{10}Y'_{20} + 3Z_{20}Y'_{10} - 3Y_{10}Z'_{20} - 4Y_{20}Z'_{10}; \qquad \text{(C-5a)}$$

$$E_3[Z_{31}] = 2Z_{10}Y''_{21} + 2Z_{11}Y'_{20} + 3Z_{20}Y''_{11} + 3Z_{21}Y'_{10}$$

$$- 3Y_{10}Z'_{21} - 3Y_{11}Z'_{20} - 4Y_{20}Z'_{11} - 4Y_{21}Z'_{10} - 4Z'_{20}; \qquad \text{(C-5b)}$$

$$E_3[Z_{32}] = 2Z_{10}Y'_{22} + 2Z_{11}Y'_{21} + 3Z_{21}Y'_{11} + 3Z_{22}Y'_{10}$$

$$- 3Y_{10}Z'_{22} - 3Y_{11}Z'_{21} - 4Y_{21}Z'_{11} - 4Y_{22}Z'_{10} - 4Z'_{21}; \qquad \text{(C-5c)}$$

$$E_3[Z_{33}] = 2Z_{11}Y'_{22} + 3Z_{22}Y'_{11} - 3Y_{11}Z'_{22} - 4Y_{22}Z'_{11} - 4Z'_{22}, \qquad \text{(C-5d)}$$

where the linear differential operator E_3 is defined by:

$$E_3 = \frac{1}{Pr}Z''_3 + 2f_0Z'_3 - 4f'_0Z_3 + 5Z'_{00}Y_3 - Z_{00}Y'_3 . \qquad \text{(C-5e)}$$

The boundary conditions for these equations are:

at $\eta = 0$: $Y_{30} = Y_{31} = Y_{32} = Y_{33} = 0$;

$$Y'_{30} = Y'_{31} = Y'_{32} = Y'_{33} = 0 ; \qquad \text{(C-6)}$$

and

$$Z_{30} = Z_{31} = Z_{32}\ Z_{33} = 0;$$

and as $\eta \to \infty$: $\frac{Y'_{30}}{\eta^4} \to \frac{[F''(0)]^2}{24}$; $Y'_{31} \to 0$; $Y'_{32} \to 0$; $Y'_{33} \to 0$ (C-7)

and $\frac{Z_{30}}{\eta^4} \to \frac{-PrF'(0)H'(0)}{8}$; $Z_{31} \to 0$; $Z_{32} \to 0$; $Z_{33} \to 0$

which follow from the coefficient function boundary conditions given in equations (B-33), (B-35) and (B-36).

APPENDIX D

DETERMINATION OF THE OUTER SERIES COEFFICIENTS

The process of determining the coefficient functions of the outer series expansions defined in equations (29) and (30) involves the solution of the ordinary linear differential equations (32); the evaluation of the resulting constants of integration; and the solution of the algebraic equations (33). The procedure is greatly simplified if the outer expansions for ψ and θ are first transformed into series with coefficients which are powers series in y^*, the coefficients of which are derived from the asymptotic forms of the f_k and g_k. This technique will facilitate the evaluation of the constants of integration significantly reduce the complexity of equations (39).

The asymptotic forms of the inner series coefficients can be written as polynomial in η with as yet undetermined coefficients as follows:

$$f_2 = a_2\eta^2 \tag{D-1a}$$

$$f_1 = A_1\eta^3 + B_1\eta^2 + C_1\eta + D_1 \tag{D-1b}$$

$$f_2 = A_2\eta^4 + B_2\eta^3 + C_2\eta^2 + D_2\eta + E_2 \tag{D-1c}$$

$$g_0 = b_1\eta \tag{D-1d}$$

$$g_1 = B_1^*\eta + C_1^* \tag{D-1e}$$

$$g_2 = B_2^*\eta + C_2^*\eta + D_2 \tag{D-1f}$$

which must satisfy the asymptotic boundary conditions specified in (B-35) and (B-36). The constants are evaluated by substituting the equations (D-1) into the original differential equations (19) and (20) and then solving the algebraic equations which appear as coefficients of like power of η. The results of this process are summarized below:

$$A_1 = \frac{-1}{6} \qquad A_2 = \frac{-b_1}{24} \qquad B_1^* = 0$$

$$B_1 = 0 \qquad B_1 = 0 \qquad C_1^* = \frac{b_1 C_1}{2a_2} \qquad \text{(D-2)}$$

$$C_1 = \text{TBD} \qquad C_2 = \frac{-C_1}{4a_2} \qquad B_2^* = 0$$

$$D_1 = \frac{-4}{3}\varepsilon^* \qquad D_2 = \text{TBD} \qquad C_2^* = \frac{-b_1 C_1}{8a_2^2}$$

$$E_2 = \frac{C_1^2}{4a} \qquad D_2^* = \frac{-b_1 D_2}{6a_2}$$

where $a_2 = \frac{1}{2} F''(0)$, $b_1 = H'(0)$ and C_1 and D_2 to be determined from application of the matching condition. This process will be outlined at the end of this appendix.

Now the equations (D-1) with the coefficients as defined in (D-2) can be substituted into stream function (15a) and temperature distribution (15b). Then if the definition of $\eta = y^*/\xi$ is invoked and all coefficients of like powers of ξ grouped together, the following expansions are obtained which are valid as y^* becomes large:

$$\psi = [a_2 y^{*2} - \frac{1}{6} y^{*3} - \frac{b_1}{24} y^{*4}] + [0]\xi$$
$$+ [C_1 y^* - \frac{C_1}{4a_2} y^{*2}]\xi^2 + [D_2 y^*]\xi^3 \qquad \text{(D-3)}$$

$$\text{and } \theta = [1 + b_1 y^*] + [0]\xi + \left[\frac{b_1 C_1}{2a_2} - \frac{b_1 C_1}{8a_2^2} y^*\right]\xi^2 + \left[-\frac{b_1 D_2}{6a_2}\right]\xi^3 \qquad \text{(D-4)}$$

With these equations in hand the final determination of the outer series coefficients can now proceed.

The first of the differential equations defined in (32a) is logarithmic and its solution has the form:

$$\psi_1 = K_1 \psi_0' \qquad \text{(D-5)}$$

Since ψ_1 is the coefficient of the linear term in the outer expansion and that coefficient in (D-3) is zero, K_1 must also equal zero, and ψ_1 has the final form:

$$\psi_1 \equiv 0 \qquad \text{(D-6)}$$

Using this equation in (D-2b) reduces it to logarithmic form with solution for ψ_2 as before:

$$\psi_2 = K_2 \psi_0' \qquad \text{(D-7)}$$

where K_2 is evaluated by equating (D-7) with the appropriate form of the ξ^2 coefficient in (D-3). The final result for ψ_2 then becomes:

$$\psi_2 = \frac{C_1}{2a_2} \psi_0' \qquad \text{(D-8)}$$

The last of the differential equations (32c) can be expressed in a simpler form using (D-6); however, its solution requires a different technique. The reduced form for (32c) is:

$$\frac{1}{2}\psi_0'\psi_3' - \frac{1}{2}\psi_3\psi_0'' = \Theta_0 + \psi_0''' \qquad \text{(D-9)}$$

Using the free convection stream function equation (9a) ψ_0''' can be written as:

$$\psi_0''' = -3\psi_0\psi_0'' + 2\psi_0'^2 - \theta_0 \qquad \text{(D-10)}$$

and by suitable algebraic manipulations in combining (D-9) and (D-10) the following differential form is obtained:

$$\left(\frac{\psi_3}{\psi_0'}\right)' = 6\left(\frac{\psi_0}{\psi_0'}\right)' - 2 \qquad \text{(D-11)}$$

Straight forward integration yields the following general solution for ψ_3:

$$\psi_3 = 6\psi_0 - 2y^*\psi_0' + K_3\psi_0' \qquad \text{(D-12)}$$

where K_3 is obtained as before with the aid of equation (D-3). Thus the particular solution ψ_3 has the following form:

$$\psi_3 = 6\psi_0 - 2y^*\psi_0' + \frac{D_2}{2a_2}\psi_0' \qquad \text{(D-13)}$$

This completes the determination of the outer expansions for ψ and θ with the exception of the constants C_1 and D_2. Since these constants appeared originally in the asmyptotic forms of f_1 and f_2 and are determined from the matching of the inner and outer series, the results of equating the universal function forms to the asmyptotic forms will yield expressions for C_1 and D_2. The following equations result from this process:

$$\text{For } f_1: \quad -\frac{1}{6}\eta_0^3 + C_1\eta_0 - \frac{4}{3}\varepsilon^* = Y_{10} + \varepsilon^* Y_{11} \qquad \text{(D-14)}$$

$$\text{and for } f_2: \quad -\frac{b_1}{24}\eta_0^4 - \frac{C_1}{4a_2}\eta_0^2 + D_2\eta_0 + \frac{C_1^2}{4a_2} =$$

$$Y_{20} + \varepsilon^* Y_{21} + \varepsilon^{*2} Y_{22} \qquad \text{(D-15)}$$

Solving for C_1 from (D-14) yields the following:

$$C_1 = C_{10} + \varepsilon * C_{11} \qquad \text{(D-16)}$$

where

$$C_{10} = \left(\frac{Y_{10}}{\eta} + \frac{1}{6}\eta^2\right),$$

and

$$C_{11} = \left(\frac{Y_{11}}{\eta} + \frac{4}{3\eta}\right)$$

A similar procedure yields the following form for D_2 obtained from (D-15):

$$D_2 = D_{20} + \varepsilon * D_{21} + \varepsilon *^2 D_{22} \qquad \text{(D-17)}$$

where

$$D_{20} = \left(\frac{Y_{20}}{\eta} + \frac{b_1}{24}\eta^3 + \frac{C_{10}}{4a_2}\eta - \frac{C_{10}^2}{4a_2\eta}\right),$$

$$D_{21} = \left(\frac{Y_{21}}{\eta} + \frac{C_{11}}{4a_2}\eta - \frac{C_{10}C_{11}}{2a_2\eta}\right);$$

and

$$D_{22} = \left(\frac{Y_{22}}{\eta} - \frac{C_{11}^2}{4a_2\eta}\right)$$

where the value η was taken as η_{end} the chosen end point of numerical integration. This completes the derivation of the outer series expansions, except to note that the constants C_{10}, C_{11}, D_{20}, D_{21}, and D_{22} are evluated numerically from the tabulated universal functions.

APPENDIX E

INTEGRAL ENERGY BALANCE ANALYSIS

In only heat transfer problem an overall thermodynamic energy balance must be satisfied. For the case of the present problem the integral energy balance takes the following form:

$$\int_0^{\infty} c_p \rho (\bar{T} - \bar{T}_{\infty})\, \bar{u} d\bar{y} = \int_0^{\bar{x}+L} g_0'' (\bar{x}) d\bar{x} \qquad \text{(E-1)}$$

The left hand side reduces to the following form with non-dimensional integrand:

$$4 c_p \rho \nu (\bar{T}_w - \bar{T}_{\infty}) \left(\frac{Gr}{4}\right)^{1/4} \int_0^{\infty} u^* \theta \, dy^* \qquad \text{(E-2)}$$

Since there are two distinct regions over which this integral is defined, it must be split into two integrals separated by the point, y^*_{edge}, where the inner and outer expansions should match. Substituting the appropriate forms for u* and θ as defined by the inner and outer series the integral (E-2) can be written as the sum of the following two integrals:

Inner region $y^* = 0$ to $y^* = \gamma$,

$$4 c_p \nu \rho (\bar{T}_w - \bar{T}_{\infty}) \left(\frac{Gr}{4}\right)^{1/4} \int_0^{\gamma} \{f_0'(\eta)\xi + [f_0'(\eta) g_0(\eta) + f_1'(\eta)]\xi^2 + [f_0'(\eta) g_1(\eta) + g_0(\eta) f_1'(\eta) + f_2'(\eta)]\xi^3\} \, dy^* \qquad \text{(E-3a)}$$

where γ is the matching point,

$\eta = \frac{y^*}{\xi}$, and $dy^* = \xi d\eta$ which transforms (D-3a) into the following:

$$4 c_p \nu \rho (\bar{T}_w - \bar{T}_{\infty}) \left(\frac{Gr}{4}\right)^{1/4} \int_0^{\gamma/\xi} \{f_0'\xi^2 + [f_0' g_0 + f_1']\xi^3 +$$

$$[f'_0 g_1 + g_0 f'_1 + f'_2]\xi^3\}d\eta \qquad \text{(E-3b)}$$

where γ depends on x.

For the outer region, $y^* = \gamma$ to $y^* = \infty$, the following integral applies:

$$4c_p\rho\nu(\overline{T}_w-\overline{T})\left(\frac{Gr}{4}\right)^{\frac{1}{4}} \int_\gamma^\infty \{F'H + \frac{C_1}{4a_2}(F'H' + F'H)\xi^2$$

$$+ [\frac{1}{6}(\frac{D_2}{2a_2} - 2y^*) + \frac{2}{3}F'H + \frac{1}{6}(\frac{D_2}{2a_2} - 2y^*)F''H]\xi^3\}dy^* \qquad \text{(E-4)}$$

The right hand integral in (E-1) also must be divided into two distinct regions, the first extending from the leading edge to the discontinuity and the second from the discontinuity to any arbitrary location above it. The following two integrals are obained:

$$\int_0^L q''_F d\overline{x} + \int_0^\xi q''_p \, d\overline{x} \qquad \text{(E-5)}$$

where q''_F is the heat flux in the undisturbed free convection region of the plate and q''_p is the heat flux above the discontinuity, both evaluated at the surface of the plate. Upon making suitable substitutions to non-dimensionalize the integrands, the following result is obtained from (D-4):

$$- 4k(\overline{T}_w-\overline{T}_\infty)\left(\frac{Gr}{4}\right)^{\frac{1}{4}} [\frac{1}{3}H'(0) + \frac{1}{3}g'_0\xi^3 + \frac{1}{4}g'_1\xi^4$$

$$+ \frac{1}{5}g'_2\xi^5] \qquad \text{(E-6)}$$

where Gr is evaluated at L and the g'_k are evaluated at the surface of the plate, $\eta = 0$.

After completing the indicated integrations in (E-3a) and (E-3b) and equating coefficients of like powers of ξ the following relationships are obtained:

$$H'(0) - H'(\gamma) = 3PrF(\gamma)H(\gamma) \qquad \text{(E-7)}$$

$$C_1 \xi^2 F'(\gamma)H(\gamma) = [F''(0)]^2 \gamma^2 \qquad \text{(E-8)}$$

$$\frac{1}{3}F''(0)H'(0)\left(\frac{\gamma^2}{\xi^2}\right) + f_1\left(\frac{\gamma}{\xi}\right) = F(\gamma)H(\gamma) - \frac{1}{3Pr}H'(\gamma)$$

$$- \frac{D_2}{12a_2}F'(\gamma)H(\gamma) + \frac{1}{3}\gamma F'(\gamma)H(\gamma) = -\frac{1}{3Pr}H'(0) \qquad \text{(E-9)}$$

The relationships can be identically satisfied only at the surface of the plate, $\eta = 0$. From this fact it can be concluded that the outer profiles are the better approximation of global behavior and will satisfy the energy balance in an integrated sense, pointwise local behavior is required near the surface of the plate the inner expansions should be used, although they cannot satisfy the integral energy balance.

LIST OF REFERENCES

1. Ede, A.J. "Advances in Free Convection," Advances in Heat Transfer, Vo. 4, p. 1-64, Academic Press, 1967.

2. Gebhart, B., Heat Transfer, 2nd edition, p. 316-407, McGraw-Hill, 1971.

3. Moore, F.K, Theory of Laminar Flows, Princeton University Press, 1964.

4. Hansen, A.G., Similarity Analysis of Boundary Value Problems in Engineering, Prentice-Hall, 1964.

5. Yang, K.T., "Possible Similarity Solutions for Laminar Free Convection on Vertical Plates and Cylinders," Journal of Applied Mechanics, Vol. 27, p. 230-236, 1960.

6. Eichhorn, R., "The Effect of Mass Transfer on Free Convection," Journal of Heat Transfer, Vol. 82, p. 260, 1960.

7. Sparrow, E. M. and Cess, R.D., "Free Convection with Blowing and Suction," Journal of Heat Transfer, Vol. 83, p. 387, 1961.

8. Parikh, P.G., Moffat, R.J., Kays, W.M., and Bershader, D., "Free Convection Over a Vertical Porous Plate with Transpiration," International Journal of Heat and Mass Transfer, Vol. 17, p. 1465, 1974.

9. Merkin, J.H., "Free Convection with Blowing and Suction," International Journal of Heat and Mass Transfer, Vol. 15, p. 989, 1972.

10. Vedhanayagam, R.A., Altenkirch, A., and Eichhorn, R., "A Transformation of the Boundary-Layer Equations for Free Convection Past a Vertical Flat Plate with Arbitrary Blowing and Wall Temperature Variations," International Journal of Heat and Mass Transfer, Vo.l 23, p. 1286, 1980.

11. Nanda, A.S., and Sharma, V.P., "Possible Similarity Solutions of Unsteady Free Convection Flow Past a Vertical Plate with Suction," Journal of the Physical Society of Japan, Vol. 17, p. 1651, 1962.

12. Soundalgekar, V.M. and Wavre , P.D., "Unsteady Free Convection Flow Past an Infinite Vertical Plate with Constant Suction and Mass Transfer." International Journal of Heat and Mass Transfer, Vol. 20, p. 1363, 1977.

13. Lal, K. "Application of Time-Dependent Suction to Free Convection Laminar Flow," Indian Journal of Physics, Vol. 43, p. 51, 1969.

14. Soundalgekar, V.M. and Pop, I. "Viscous Dissipation Effects on Unsteady Free Convective Flow Past an Infinite Vertical Porous Plate with Variable Suction," International Journal of Heat and Mass Transfer, Vol. 17, p.85, 1974.

15. Na, T.Y., "Numerical Solution of Natural Convective Flow Past a Non-isothermal Vertical Flat Plate," Applied Science Research, Vol. 33, p. 519, 1978.

16. Meena, B.K. and Nath, G., "Nonsimilar Laminar Free Convection Flow Along a Non-isothermal Vertical Plate," Journal of Heat Transfer, Vol. 100, p. 163, 1978.

17. Goldstein, S., "Concerning Some Solutions of the Boundary Layer Equations in Hydrodynamics," Proceedings of the Cambridge Philosophocal Society, Vol. 26, p. 1, 1929.

18. Yang, K.T., "Laminar Free Convection Wake Above a Heated Vertical Plate," Journal of Applied Mechanics, Vol. 31, p. 131, 1964.

19. Kelleher, M.D., "Free Convection From a Vertical Plate with Discontinuous Wall Temperature," Journal of Heat Transfer, Vol. 93, p. 349, 1971.

20. Nachtstein, P.R. and Swigert, P. "Satisfaction of Asymptotic Boundary Conditions in Numerical Solution of Systems of Nonlinear Equations of Boundary Layer Type, NASA TN D-3004, 1965.

INITIAL DISTRIBUTION LIST

		No. Copies
1.	Defense Technical Information Center Cameron Station Alexandria, Virginia 22314	2
2.	Library, Code 0142 Naval Postgraduate School Monterey, California 93940	2
3.	Department Chairman, Code 69 Department of Mechanical Engineering Naval Postgraduate School Monterey, California 93940	1
4.	Professor M.D. Kelleher, Code 69 Department of Mechanical Engineering Naval Postgraduate School Monterey, California 93940	1
5.	Professor B. Gebhart, Code 69 Department of Mechanical Engineering Naval Postgraduate School Monterey, California 93940	1
6.	Professor K.T. Yang Department of Aerospace and Mechanical Engineering University of Notre Dame Notre Dame, Indiana 46556	1
7.	LCDR William Schiesser 300 Glenwood Circle, Apt. 159 Monterey, California 93940	1

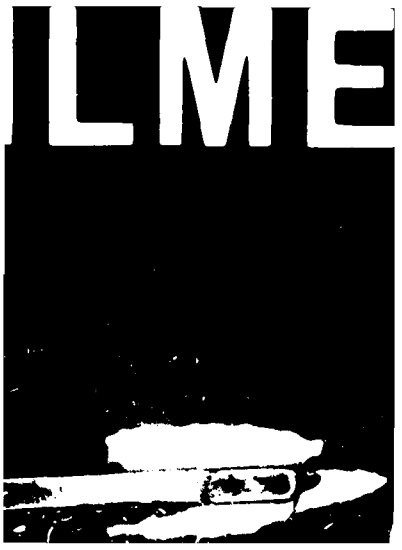
LME